Seeing through the Effects of Crustal Assimilation to Assess the Source Composition Beneath the Southern Lesser Antilles Arc

Rachel Bezard[1,2], Simon Turner[2], Jon P Davidson[1] Colin G Macpherson[1], Jan M Lindsay[3]

[1] Durham Geochemistry Centre, Department of Earth Sciences, Durham University, South Road, Durham DH1 3LE, UK

[2]Department of Earth and Planetary Sciences, Macquarie University, University Avenue, Macquarie Park NSW 2113, Australia

[3] School of Environment, The University of Auckland, Symonds St, Auckland, 1142, New Zealand

Corresponding author:

Name: Rachel Bezard
E-mail: bezard@uni-muenster.de
Present address: Institut für Planetologie, Westfälische Wilhelms-Universität Münster, Wilhelm-Klemm-Str. 10, 48149 Münster, Germany
Tel: 0491752120688
Fax: 0492518336301

Running title: Seeing through the effects of crustal assimilation

ABSTRACT

Assessing the impact of crustal assimilation on the composition of oceanic arc lavas is important if source composition is to be correctly interpreted. This is particularly the case in the Lesser Antilles where lavas encompass a very large range in radiogenic isotope ratios. Here we present new $^{176}Hf/^{177}Hf$ and trace element data for a suite of samples from St Lucia, in the southern Lesser Antilles arc, where assimilation of sediments located within the arc crust has been shown to significantly impact Sr-Nd-Pb isotope compositions. We show that a high rate of assimilation (r = 0.8) of sediment is responsible for the co-variation of Th/Th*, La/Sm, $^{87}Sr/^{86}Sr$, $^{206/207/208}Pb/^{204}Pb$, $^{143}Nd/^{144}Nd$ and $^{176}Hf/^{177}Hf$ toward extreme "continental" compositions. Lavas that escaped sediment assimilation have a typical oceanic arc signature and provide the best reflection of mantle source characteristics beneath St Lucia. They display similar Ba/Th, La/Sm and Nd isotopic composition but slightly more radiogenic Sr and Pb than lavas further north in the arc. Calculations indicate that addition of less than 2 % of the local bulk subducting sediments or less than 3.5% of sediment partial melts or fluids to the mantle can explain these compositions; these estimates are similar to those previously obtained for the northern arc. Therefore, after removal of the effects of sediment assimilation, St Lucia lavas have only slightly more radiogenic Pb and perhaps Sr isotope signatures compared to the northern islands and this can be attributed to differences in the isotopic composition of the subducting sediment rather than greater sediment input, as has been previously proposed. Comparison of St Lucia with the other southern Lesser Antilles islands suggests similar source compositions exist beneath Martinique, St Vincent and maybe Bequia, while a more "continental" source might characterize Ile de Caille, Kick'em Jenny and Grenada.

Key words: Lesser Antilles, assimilation, oceanic arc, sediment, St Lucia

INTRODUCTION

Global arc studies have shown that oceanic arcs can be divided into two groups based on their trace element and radiogenic isotope compositions (Hawkesworth et al., 1993). The first group comprises, amongst others, Tonga, Mariana, South Sandwich and the Aleutian arcs which are characterised by compositions often termed "typical oceanic arcs" that have a relatively narrow range of Sr, Nd, Hf and Pb isotope compositions that differ only slightly from mid-oceanic ridge basalts (MORBs). Oceanic arcs from the second group (e.g., Java, Banda, Philippines) have more heterogeneous compositions comprising very "continental" isotopic compositions (more radiogenic Sr and Pb isotope ratios with less radiogenic Nd and Hf isotopicratios). They also have higher light versus middle and heavy rare-earth elements ratios (L/M-HREE) and lower ratios of large-ion lithophile elements versus high field strength elements (LILE/HFSE; e.g. Ba/Th), similar to continental arcs (Hawkesworth et al., 1993; Woodhead et al., 2001). Understanding the origin of the "continental" signature observed in some oceanic arcs is important to assess the crust production and recycling at subduction zones (Davidson & Arculus, 2006).

The Lesser Antilles arc (Fig. 1) is a well-known example of an oceanic arc which has a "continental" signature (White & Dupré, 1986; Davidson, 1987; Macdonald et al., 2000; Fig. 2). Lavas with "continental" Sr, Nd, Hf and Pb isotope compositions are restricted to islands from the central-southern segments of the arc, while the northern islands display "typical oceanic arc" compositions. Relative to the northern lavas, the continental signature observed in some of the lavas in the southern arc could be explained by the contamination of the mantle wedge by greater amounts of, or more continental-like, sediments from the subducting slab.(White & Dupré, 1986; Labanieh et al., 2010; 2012). However, sediment assimilation has been shown to be significant in Martinique (e.g. Davidson & Harmon, 1989) and St Lucia (Bezard et al., 2014), which are the two

65 islands displaying the largest isotopic heterogeneities. Therefore, in order to interpret the source
66 compositions in this region, an understanding of the impact of sediment assimilation is required.
67 Such an exercise has been performed for Martinique, where Davidson & Wilson (2011) stripped
68 off the effects of sediment assimilation and other differentiation processes by back-extrapolating
69 major and trace element and isotope differentiation trends to a SiO_2 composition likely to
70 characterize the primary magmas of the suite (SiO_2 = 48 wt. %). They extended their comparative
71 studies to other islands and proposed that the chemical and isotopic compositions of the mantle
72 source beneath Martinique and St Vincent, both from the southern arc, are not dissimilar to the
73 source beneath the northern islands magmas. This suggests that the north-south trace element and
74 isotopic variations could be almost entirely produced by sediment assimilation.

75 In order to test this hypothesis, we performed a detailed study of lavas from St Lucia. Here,
76 the filtering of sediment assimilation cannot be performed using the back-extrapolation method of
77 Davidson & Wilson (2011), because differentiation trends are harder to establish. However, in St
78 Lucia, very good constraints on which lavas are affected by sediment assimilation are available
79 from a study of $\delta^{18}O$ in phenocrysts (Bezard et al., 2014). This allows comparison of the
80 compositions of lavas that are significantly affected by sediment assimilation and those that are
81 negligibly affected in order to isolate which elements and isotopes were modified by sediment
82 assimilation. This exercise was carried out for Sr, Pb and Nd isotopes by Bezard et al. (2014) who
83 showed that these elements were very sensitive to sediment assimilation. However, the constraint
84 of the composition and amount of sediment assimilated and the characterization of the mantle
85 source compositions were beyond the scope of Bezard et al. (2014) contribution. Here we
86 investigate the overall impact of sediment assimilation using new Hf isotope and trace element
87 compositions coupled with published Sr, Pb and Nd isotopes data in order to constrain (1) the

88 nature of the assimilant and (2) St Lucia mantle source characteristics and compare them with
89 other Lesser Antilles islands.

90

GEOLOGICAL SETTING

The 800 km long Lesser Antilles arc (Fig. 1a) results from subduction of the North American Plate under the Caribbean Plate (Fig. 1a). The arc was initiated in the late Oligocene (Germa et al., 2011) and is currently active. It exhibits major geochemical and isotopic differences from north to south. Northern islands are characterised by tholeiitic and calc-alkaline volcanic rocks with very limited isotope and trace element ratios variations (e.g. Sr-Nd isotopes; Fig. 2). In contrast, the central and southern sections of the arc have erupted a wider range of magma types, extending to alkaline lavas. These central-southern magmas are characterised by large isotope and trace element ratio variations, ranging from compositions similar to those of the northern islands to compositions more similar to continental crust (Fig. 2). This geographic variation has been suggested to reflect physical variation of the arc system (e.g. Van Soest et al., 2002) including basement heterogeneity (Speed & Walker, 1991; Aitken et al., 2011), age and thickness variations of the volcanic sequences (McCann & Sykes, 1984; Bouysse & Westercamp, 1990), and changes in nature and amount of sediment in the trench from north to south (Carpentier et al., 2008).

St Lucia is located between Martinique and St Vincent (Fig. 1a) and belongs to the central section of the arc as defined by Macdonald et al. (2000). Current activity is focused within the Qualibou depression (Fig. 1b), a large sector collapse in the south-west of the island (Lindsay et al., 2013). St Lucia rocks can be separated into two main groups based on age constraints.

Pre-Soufrière Volcanic Complex

The first and oldest group, termed the Pre-Soufrière Volcanic Complex (Pre-SVC) consists dominantly of eroded basalt, basaltic andesite and andesite centres, with only one rhyolite flow (OAS, 1984). Rocks in this group are present across the island (Fig. 1b) and have been dated by

K-Ar to between 15-18 Ma and 3.13 Ma by Briden et al. (1979), Aquater, (1982) and De Kerneizon et al. (1983). Two Pre-SVC basaltic andesite flows, cropping out in the Qualibou depression, in the south-west of the island were initially dated by K-Ar between 6.1 ± 0.6 and 6.5 ± 0.6 Ma at Jalousie (Aquater, 1982) and 5.61 ± 0.25 Ma at Malgretoute (Briden et al., 1979). The same flows were more recently dated, using the same method, at 1.10 ± 0.02 and (Jalousie) and 6.64 ± 0.12 Ma (Malgretoute) by Samper et al. (2008). Pre-SVC lavas can been separated into two subgroups on the basis of their Sr-Nd isotopic signatures (Bezard et al., 2014). The first, and main, subgroup (Pre-SVC1) has typical oceanic arc signatures in terms of $^{87}Sr/^{86}Sr$ and $^{143}Nd/^{144}Nd$ (0.70411-0.70439 and 0.51295-0.51298 (εNd = +6.01 to +6.73) respectively). Pre-SVC1 lavas also have Pb isotopes close to typical oceanic arc signatures ($^{206}Pb/^{204}Pb$, $^{207}Pb/^{204}Pb$ and $^{208}Pb/^{204}Pb$ range from 19.291-19.341, 15.747-15.748, 38.96-39.11, respectively). According to mineral $\delta^{18}O$ data, which overlap or plot very close to the mantle range (unlike the rest of the lavas on the island), this group is thought to be minimally affected by assimilation of sediment during ascent (Bezard et al., 2014) and is therefore the closest representative of St Lucia primary magma. However, Pre-SVC1 lava compositions may not entirely reflect mantle source characteristics. Indeed, Bezard et al. (2015) used Os isotopes to suggest that even the most mafic lavas that escaped sediment assimilation, such as Pre-SVC1, could still have been partly modified by assimilation of lower crust during their early storage.The second subgroup (Pre-SVC2) has more “continental” Sr-Nd isotopic compositions (0.70611-0.70622 and 0.51251-0.51258 (εNd = -2.59 to -1.14), respectively; Pb isotopes were not analysed) that vary with indexes of differentiation such as SiO_2 and with mineral $\delta^{18}O$ values, indicating larger contributions of assimilated sediment within the arc crust.

Soufrière Volcanic Complex

135 The second and younger group of volcanic rocks on the island is the Soufrière Volcanic Complex
136 (SVC). It comprises eroded high-silica andesite and dacite volcanic centres with associated
137 volcaniclastic units (Fig. 1b) dated between 3 Ma to Recent (Lindsay et al., 2013). Lindsay et al.
138 (2013) separated the activity of the SVC into three different periods. The first period of eruption
139 occurred between 3 Ma and ca. 250 Ka and produced andesitic stratovolcanoes of the SVC as well
140 as andesitic to dacitic pyroclastic deposits. This was followed by a major sector collapse between
141 250-100 Ka resulting in the Qualibou depression and uncovering the shallow parts of the SVC
142 basement made of mafic Pre-SVC1 units (e.g. SL-83-25 basaltic andesite; Bezard et al., 2014).
143 Finally, dacitic domes and pyroclastic deposits were emplaced in the region of the depression
144 during two main eruptive periods: 100-50 Ka and 20 Ka-present.

145 The SVC plumbing system was investigated by Schmitt et al. (2010) who proposed an
146 evolutionary model based on U-Th and (U-Th)/He zircon ages. Their results indicated episodic
147 thermal and mechanical rejuvenation within a complex of a long-lived intermediate mid-crustal
148 plutons under the Qualibou depression. SVC lavas display extreme Sr-Pb-Nd isotopic
149 compositions, typical of continental crust, with high Sr-Pb ($^{87}Sr/^{86}Sr$ = 0.70754-0.70906;
150 $^{206}Pb/^{204}Pb$ = 19.721-19.797, $^{207}Pb/^{204}Pb$ = 15.826-15.846, $^{208}Pb/^{204}Pb$ = 39.438-39.528) and low
151 Nd isotopic ratios (0.51210-0.51226; εNd = -10.67 to -7.36; Bezard et al., 2014). This shift to
152 continental signatures (compared to Pre-SVC lavas) correlates with increases in SiO_2 and is
153 associated with high $\delta^{18}O$ values in phenocrysts, supporting sediment assimilation during magma
154 differentiation (Bezard et al., 2014). The occurrence of the most continental signatures in the SVC
155 suggests a correlation between the factors responsible for the development of the silicic complex
156 and the occurrence of major crustal assimilation. However, the understanding of these factors is
157 beyond the scope of this contribution.

SAMPLING AND ANALYTICAL PROCEDURES

Samples

A total of 32 lava and pumice samples from St Lucia were selected to encompass the whole range of major element compositions in both the Pre-SVC (basalt to rhyolite) and the SVC (high silica andesite to dacite). These were analysed for their trace elements and 26 were selected for Hf isotope analyses. All the samples have been previously analysed for major elements (Davidson, 1984; Lindsay et al., 2013) and Sr-Nd-Pb isotopes (Bezard et al., 2014) on the same hand samples. Furthermore, 2 samples previously analysed for trace elements (Lindsay et al., 2013) by LA-ICPMS were re-analysed to maintain internal consistency.

Trace elements

Thirty samples were analysed at Durham University and two samples analysed at the Geochemical Analysis Unit (GAU) at Macquarie University.

At both Durham and Macquarie, samples were analysed twice: once using rock powder and once on fused glass to obtain Zr, Hf, U and Ti concentrations in zircon-bearing rocks. Although Ti concentrations were already obtained by X-ray fluorescence (XRF; Davidson, 1984; Lindsay et al., 2013), we re-analysed it on fused glasses for consistency. At Durham trace elements were analysed in solution by inductively coupled plasma mass spectrometry (ICP-MS) using the Thermo Scientific X-Series Element 2 instrument using the technique described by Ottley et al. (2003). Rock powders (0.1g) were digested in a HNO_3/HF mixture. After digestion, samples were dried and re-dissolved in HNO_3 twice. The sample was then dissolved in dilute HNO_3 before analysis. In all zircon-bearing felsic samples, rock powders were also fused with lithium tetraborate flux and subsequently crushed in an agate ball mill and analysed again in solution

following the technique described by Ottley et al. (2003). For the latter analyses, data were blank corrected using processed fused flux and fused fluxed standards for calibration. At Macquarie, rock powders were analysed in solution using an Agilent 7500 Series ICP-MS instrument. As in Durham, the rock powders were fused with Lithium tetraborate flux to obtain Zr, Hf, U and Ti concentrations. Fused disks were analysed using a NewWave UP-213 laser ablation system linked to an Agilent 7700 Series ICP-MS system. Ablation of the samples was performed in a helium-filled chamber using a frequency of 5 Hz and an ablation spot size of 50 μm or a line 240 μm long. CaO from XRF analyses was used as an internal standard. At both Durham and Macquarie Universities, the reproducibility was checked by analysing three replicates of the same sample in each batch. Relative standard deviation between the three replicates of each batch was less than 3% for all elements presented. The inter-lab reproducibility of the data was verified by analysing basaltic standards BHVO-1 or BHVO-2 (which are identical for the elements presented, except for Pb) in every batch of sample (results are provided in the Supplementary file 1). Differences between our measured BHVO-1 concentrations in every batch and the Georem prefered values (http://georem.mpch-mainz.gwdg.de) are less than 5% for all elements presented.

Hf isotopes

For Hf isotopes, 20 samples were analysed by multicollector-inductively coupled plasma-mass spectrometry (MC-ICP-MS) using the Thermo Scientific Neptune instrument at Durham and six samples were analysed using the same method but using a Nu plasma instrument at Macquarie. At Durham, Hf was first collected from Sr-spec resin columns used to separate Sr and Pb from the sample (Bezard et al., 2014). Hf was then separated from other rare earth elements and Ba using a cationic resin (AG50W X-8) and from Ti using AG1-X8 anion-exchange resin. At Macquarie, Hf was first collected from cation exchange resin columns (AG 50W-X8) where it was separated from

the Sr and Nd cuts (Bezard et al., 2014). The Hf cuts were then purified in two stages using AG1-X8 and AG50W-X8 anion- and cation-exchange resins respectively. At both Durham and Macquarie, the measurements were made in static-collection mode and mass bias was corrected using $^{179}Hf/^{177}Hf$ of 0.7325 and an exponential law. At Durham, ten JMC475 solutions were analysed during the analytical session. The average $^{176}Hf/^{177}Hf$ was 0.282144 ± 0.000006 (2SD) and was then used to correct for $^{176}Hf/^{177}Hf$ of all processed samples and standards assuming a JMC475 standard value of 0.282160 (Nowell et al., 1998). The $^{176}Hf/^{177}Hf$ of the two international rock standards BIR-1 and BHVO-1 analysed were 0.283239 and 0.283105, respectively. At Macquarie, four JMC475 solutions were analysed during the analytical session. The average was 0.282162 ± 0.000017 (2SD) which is in very good agreement with the accepted value. The $^{176}Hf/^{177}Hf$ of BHVO-1 was 0.283107, which is in excellent agreement with Weis et al. (2007) (0.283106 ± 12; 2SD) and with the BHVO-1 composition obtained in Durham which demonstrates the excellent inter-lab reproducibility.

RESULTS

New trace element and Hf isotope data are presented in Table 1 along with the corresponding major elements, Sr, Nd and Pb isotope ratios (Bezard et al., 2014).

Trace elements

Pre-SVC and SVC lavas and pumices display classic arc trace element signatures with enrichment in LILE and depletion of HFSE relative to the REE. However, in detail, distinctions exist, not only between the Pre-SVC and SVC volcanic rocks, but also between the Pre-SVC1 and Pre-SVC2 samples (Fig. 3). Extended trace element patterns presented in Fig. 3b, d and f clearly show that the main differences amongst the lavas are found in L/M-HREE and Th/Ba and Th/U. When

normalised to chondrite, Pre-SVC1 lavas (Fig. 3a, b) display negative Th anomalies with Th/Th*(Th_N / ((Ba_N + U_N)/2)) between 0.45-0.71, and a flat REE pattern with La/Sm, La/Yb, Dy/Dy* (= Dy_N / ($La_N^{4/13}$*$Yb_N^{9/13}$)) and Dy/Yb ranging between 1.4-1.9, 1.5-2.3, 0.87-1.07 and 1.47-1.65 respectively. They also display variable Ba/Th (98-200). Compared to Pre-SVC1, Pre-SVC2 (Fig. 3c and d) lavas have slightly higher Th/Th* (0.80-0.84) lower Ba/Th (85-95) and slightly enriched LREE/M-HREE with La/Sm, La/Yb, Dy/Dy* and Dy/Yb ranging between 2.5-3, 2.9-3.5, 0.79-0.85 and 1.58-1.6, respectively. Samples from the SVC (Fig. 3e, f) plot within a very narrow compositional range. They have negligible Th anomalies (Th/Th*=0.87-1.08), low Ba/Th (58-79) and a REE pattern highly enriched in LREE compared with M-HREE, with La/Sm, La/Yb, Dy/Dy* and Dy/Yb between 5.6-8.2, 10.5-18.4, 0.47-0.59, 1.51-1.72, respectively.

Hf isotopes

Hf isotope ratios (Fig. 4a) also differ between the three groups defined by the trace element concentrations and the Sr-Nd-Pb isotopes (Fig. 4b). Pre-SVC1 samples have typical oceanic arc isotopic signatures with $^{176}Hf/^{177}Hf$ ranging between 0.283027 and 0.283156 (εHf = +9.02 to +13.57). Pre-SVC2 lavas extend toward some more radiogenic signatures with $^{176}Hf/^{177}Hf$ ranging between 0.282755 and 0.282802 (εHf = -0.60 to +1.08). Finally, all the SVC samples have very radiogenic signatures with $^{176}Hf/^{177}Hf$ between 0.282419 and 0.282603 (εHf = -14.11 to -5.98).

SEDIMENT ASSIMILATION CONTROL ON MAGMA COMPOSITIONS

Impact of sediment assimilation on $^{176}Hf/^{177}Hf$

Two principal factors are capable of producing variations in the isotopic compositions of arc magmas: (1) variation in the nature and amount of subducted slab component(s) added to the source (from current or previous subduction) and (2) changes in the amount of crust assimilation.

Bezard et al. (2014) showed that on St Lucia, Sr-Pb-Nd isotope variations correlate with indices of differentiation and also with a clear departure from the mantle range of phenocryst $\delta^{18}O$ values providing unequivocal evidence for sediment assimilation. Sediments with continental Sr, Nd and Pb isotopes also typically have continental Hf isotopes (e.g. Vervoort et al., 1999), therefore Hf isotopes are expected to be affected by assimilation too.Hf isotope ratios decrease from Pre-SVC1 to the SVC lavas and correlate with the variations toward more continental signatures observed in Nd, Sr, Pb and O isotopes, consistent with control of Hf isotopes by sediment assimilation. . This is confirmed when Hf isotopes are plotted against SiO_2 (Fig. 5a) revealing similar variations to that shown by $^{143}Nd/^{144}Nd$ versus SiO_2 (Fig. 5b). Pre-SVC1 shows negligible variation in $^{176}Hf/^{177}Hf$ trend while Pre-SVC2 and SVC volcanic rocks show a clear negative correlation. The absence of correlation between radiogenic isotope compositions and indices of differentiation in the Pre-SVC1 lavas suggests closed system fractional crystallisation, while the correlation formed by SVC and Pre-SVC2 samples argues for assimilation during differentiation. Since the two trends back project toward a similar end member, the two groups seem to share a similar primitive/parental magma, as suggested by Sr-Nd isotopes (Fig. 5b, c).

Impact of sediment assimilation on trace elements

The main trace element variations observed amongst the St Lucia volcanic rocks are tightly linked with the isotopic variations shown to result from sediment assimilation and may therefore be controlled by the same process. Indeed, similar to radiogenic isotopes, no La/Sm and Th/Th* variation exists with increasing SiO_2 in Pre-SVC1 lavas, while Pre-SVC2 and SVC volcanic rocks form a trend toward higher Th/Th* and La/Sm with increasing SiO_2, similar to the isotope ratios (Fig. 5e, f). However, unlike radiogenic isotopes, trace elements are affected by mineral fractionation. Therefore, the increases in La/Sm and Th/Th* observed in St Lucia volcanic rocks,

which are tightly linked with the assimilation event, do not necessarily reflect the composition of the assimilant and might instead (or in part) be produced by a change in the fractionating mineral assemblage. For example, a change in the fractionating assemblage could be caused by a change in water content of the magma produced by the dehydration of the assimilant during its incorporation. In order to constrain the impact of sediment assimilation on the trace element variations observed between Pre-SVC1, Pre-SVC2 and SVC volcanic rocks, the effects related to fractional crystallisation alone need to be quantified first. To do so, determination and quantification of the phases involved in fractionation of the Pre-SVC1 basalt liquid to produce the SVC lavas was undertaken using major element concentrations. A Pre-SVC1 basalt (SL-83-44) was chosen as a starting composition since this represent the most mafic end-member on the island and both the trends formed by Pre-SVC1 and by Pre-SVC2 and SVC back project toward this composition. Using partition coefficients, we subsequently model La/Sm and Th/Th* variations due to mineral fractionation and then compare these with the observed SVC compositions.

Determination of the fractionating assemblage using major elements

In the absence of crustal assimilation, the major element compositions of magmas are only controlled by the composition of the primitive magma and the phases removed by crystal fractionation. In a case where crustal assimilation is significant and the assimilant has a distinct major element composition to the magma, the differentiation trend might show a clear change at the onset of assimilation.

When plotted on an AFM diagram (Fig. 6a), all of the Pre-SVC1 samples plot in the tholeiitic field (Irvine & Baragar (1971) boundary) while the SVC samples all belong to the calc-alkaline field and Pre-SVC2 lavas plot at the boundary between the two or in the calc-alkaline field. Therefore, samples that experienced increasing sediment assimilation were progressively

displaced toward the calc-alkaline field. Such observation is consistent with experiments of Grove et al. (1982) which show that assimilation of crustal material can produce a calc-alkaline trend from tholeiites. However, when major element oxide variations are plotted against SiO_2 (Fig. 6b-g), no significant change in the differentiation trends between Pre-SVC and SVC samples are observed. In the Pre-SVC samples, most major element oxides show a general linear trend from basalt to rhyolite, although scatter exists in the data. The absence of inflections indicates that there was no sudden major modal abundance changes in the fractionating assemblages, nor sudden addition of assimilant with a very distinct composition. The SVC compositional trends are linear and overlap with the Pre-SVC trends for CaO, TiO_2, MgO and K_2O, however, the SVC have slightly higher Al_2O_3 and lower FeOt (total Fe as FeO). This slight difference might be either due to a change in the phases of the fractionating assemblage and/or in the amount of the phases fractionated or due to assimilation.

For all St Lucia samples, > 93% of CIPW normative minerals plot in the quartz-feldspar-orthopyroxene-clinopyroxene tetrahedral system and all Pre-SVC and SVC samples could have been differentiated from the most mafic Pre-SVC sample (SL-83-44) by fractionation of clinopyroxene + orthopyroxene + plagioclase . SVC samples follow the Pre-SVC cotectic and Pre-SVC and SVC andesites have very similar normative compositions. Although CIPW norms represent a dry system, the results are in very good agreement with the mineralogical assemblages observed in thin section. All the Pre-SVC lavas have phenocryst assemblages that are comprised of plagioclase, clinopyroxene, orthopyroxene with minor ilmenite and resorbed olivine. The SVC andesite phenocryst assemblages are mainly comprised of plagioclase, orthopyroxene with minor resorbed quartz. Finally, the SVC dacites contain some or all of the phases plagioclase, orthopyroxene or cummingtonite, quartz, biotite and hornblende microphenocrysts. Plutonic

316 inclusions found in some of the SVC volcanic rocks have the same mineral assemblage as their
317 host but in different modes.

318 In order to further test whether the Pre-SVC1 and SVC andesites can both be produced by
319 fractionation of similar phases from the most mafic Pre-SVC1 lava and to constrain the modal
320 abundances of such phases, we performed least-squares modelling using an Excel-based version
321 of XTLFRAC (Stormer & Nicholls, 1978). We used the most mafic Pre-SVC1 lava (SL-83-44) as
322 a starting composition, and high-silica andesite (with similar SiO_2) from both the Pre-SVC and the
323 SVC groups for the resultant magmas. For the possible fractionating assemblages, we explored
324 combinations of all different phase compositions found in both the Pre-SVC mafic-andesitic
325 samples and the SVC andesitic mineral assemblages (and in both volcanic rocks and xenoliths).
326 Since amphibole is not present in either the Pre-SVC or SVC andesites, we used the composition
327 of high-Ca and low-Ca hornblende micro-phenocrysts found in some SVC dacites and in the
328 plutonic xenoliths. In the model, we used combinations of 9 major elements oxides and 4 phases.
329

330 The least squares models are presented in Fig. 6b-g. A very good fit of $\sum R^2 = 0.05$ was
331 obtained by fractionating the observed plagioclase + clinopyroxene + orthopyroxene + ilmenite
332 assemblage for the Pre-SVC andesite (Table 2 model #3). Using the same phenocryst assemblage,
333 but with orthopyroxene having slightly lower MgO and plagioclase with lower anorthite, a very
334 good $\sum R^2$ was obtain for the SVC andesite ($\sum R^2 = 0.03$) (Table 2, model #1).

335 No least squares solution that involves fractionation of amphibole (using either the SVC
336 dacite or granitoid amphibole composition) or olivine produced a residual melt with the Pre-SVC
337 andesite composition. For the SVC andesite, a good fit for an amphibole-bearing assemblage could
338 be obtained, however, it only involved fractionation of less than 1% of amphibole (Table 2, model

#2). The fits were not improved when phase compositions from the plutonic xenolith assemblages were used.

Impact of the fractionating assemblage on the trace element variations

Using the most mafic Pre-SVC1 lava (SL-83-44) as a starting composition, the partition coefficients presented in Table 3 and the Rayleigh fractionation equation, we calculated the impact of fractionation of the least squares model assemblages on Th/Th* and the REE ratios of the magmas. Results are presented in Table 2.

Th/Th;* The results show that none of the fractionating assemblages obtained from the least squares models can produce a significant increase in Th/Th* (Fig. 5f). Residual melts from least square models #1 and #2 have Th/Th* of 0.72, while the residual melt from model #3 has a ratio of 0.71. Therefore, Th/Th* of all residual melts are very similar or identical to the starting melt composition (SL-83-44; Th/Th* = 0.71), and indicate that Th/Th* remains almost constant during fractionation. Th/Th* obtained are far lower than the ratio observed in the SVC andesite of 0.96, suggesting that the difference needs to be accounted for by sediment assimilation. Because the decrease of the Th anomaly in the Pre-SVC2 and the SVC lavas relative to Pre-SVC1 lavas is due to an increase in Th instead of a decrease in Ba and U (Fig. 3), we argue that the assimilant possesses higher Th/Ba and Th/U than the Pre-SVC1 lavas.

Ba/Th is often used to constrain the amount of fluid versus sediment from the subducting slab in the mantle wedge source. On St Lucia, the increase in Th reduces the Ba/Th of the Pre-SVC2 and SVC volcanic rocks by 16-25% and 32-39% respectively. We therefore suggest that a correlation between Th/Th* and SiO_2 should be precluded before using a proxy such as Ba/Th for source characterisation. Pre-SVC1 samples do not show any correlation of Th anomaly with SiO_2,

361 therefore, the large range of Ba/Th should represent source variations, if no other cryptic
362 assimilation has occurred.

363 *REE;* As noted by Davidson et al. (2007), during magma differentiation, fractionation of
364 olivine and plagioclase does not significantly affect the L/M-HREE. Although pyroxene
365 fractionation can increase the L/M-HREE of the magma slightly, amphibole and garnet
366 fractionation (including amphibole crystallising by reaction-replacement of clinopyroxene; Smith,
367 2014) produce larger changes in this ratio.

368 The fractionating assemblages obtained from least squares modelling provide no
369 suggestion of garnet fractionation during differentiation from Pre-SVC1 basalt to Pre-SVC1 or
370 SVC andesites. The absence of garnet fractionation is confirmed by the lower Dy/Dy* of the SVC
371 (0.47-0.59) and Pre-SVC2 (0.79 vs 0.85) volcanic rocks compared to Pre-SVC1 basalt (0.97).
372 Indeed, garnet preferentially incorporates HREE followed by MREE and LREE while amphibole
373 and pyroxene preferentially incorporate MREE followed by HREE and LREE (Davidson et al.,
374 2013). The Dy/Yb and Dy/Dy* of the most mafic Pre-SVC1 lava (SL-83-44) is chondritic,
375 therefore, any garnet fractionation during differentiation of such magma would produce magma
376 with Dy/Dy* > 1. However, Dy/Dy* is < 1 for Pre-SVC2 and SVC lavas, which indicates that
377 fractionation of garnet from the more primitive St Lucia basalt is very unlikely to be involved in
378 their genesis. Therefore, only pyroxene and amphibole fractionation are capable of increasing
379 L/M-HREE in the Pre-SVC1 and SVC andesites.

380 As for Th/Th*, fractionation of the least squares models mineral assemblages obtained for
381 the production of Pre-SVC1 andesites (SL-83-41; La/Sm = 1.9; La/Yb = 2.3) and SVC andesites
382 (SL-83-17; La/Sm = 5.7; La/Yb = 11.3) from the differentiation of Pre-SVC1 basalt (SL-83-44;

383 La/Sm = 1.65; La/Yb = 1.74) did not result in any significant increase in La/Sm in the residual
384 melt (Fig. 5e). Indeed, results show that fractionation of assemblages #1 and #3, which are
385 amphibole-free, produced a residual melt with L/M-HREE similar to the observed Pre-SVC1
386 andesitic ratios (SL-83-41; La/Yb = 2.30; La/Sm = 1.90) with La/Yb and La/Sm of 2.19-2.31 and
387 1.82-1.90 respectively. Fractionation of the amphibole-bearing assemblage (0.9% hornblende; #2),
388 also yields low La/Yb or La/Sm (2.29 and 2.02; Fig. 5e). These low L/M-HREE indicate that the
389 increase in La/Sm (and La/Yb) observed in the SVC volcanic rocks cannot be due to mineral
390 fractionation but rather reflects the characteristics of the assimilant.

391 **COMPOSITION OF THE SEDIMENT ASSIMILATED**

392 **Major and trace elements**

393 The limited differences in major element compositions between Pre-SVC and SVC lavas of similar
394 MgO can be easily accounted for by fractional crystallisation alone. This indicates that, if
395 significant crustal assimilation occurred in the SVC, addition of the assimilant must have had a
396 similar effect on major element compositions of the magma as the removal of the crystallising
397 assemblage. Terrigenous sediments derived from continental crust could have appropriate
398 compositions since they are andesitic to silicic on average (e.g. Plank and Langmuir, 1998). Many
399 of the local sediments fulfill such criteria. This is true of the pelagic and radiolarian clays drilled
400 on the subducting plate at Site DSDP site 543 (see Supplementary data file 2 for sedimentary
401 sequences description) and for the terrigenous claystones and sandstones from Barbados
402 sediments, both of which originate from the South American craton (Carpentier et al., 2009).
403 Contamination by carbonate-rich sediments, such as grey marl and chalk ooze (Units 1 and 2;
404 Mean CaO=30 wt. %) or the black shales (Unit 3; Mean CaO = 33 wt. %) intersected at DSDP site
405 144 (see Supplementary data file 2), seems less likely since their assimilation should produce a

406 shift in the differentiation trend of CaO in the Pre-SVC2 and SVC volcanic rocks compared to Pre-
407 SVC1 lavas, which is not observed (Fig. 6). Alternatively, it could be argued that the effect on
408 CaO of assimilation of such sediment could be buffered by fractionation of large quantities of
409 calcic magmatic phases such as plagioclase and clinopyroxene.

410 Local sediments having the assimilant trace element features are abundant since high
411 La/Yb or La/Sm ratios and high Th/Ba and Th/U relative to Pre-SVC1 lavas characterise sediments
412 from both DSDP sites 543, 144 and from Scotland formation of Barbados (not the Oceanic
413 formation which comprises tephra) (Carpentier et al., 2008; 2009).

414 **Isotopic composition and rate of sediment assimilation**

415 AFC modelling performed in the 1980's and 1990's to explain the extreme isotope signatures of
416 the Lesser Antilles lavas highlighted the need for the assimilant to have very radiogenic Pb, but
417 failed to find local sediment with such composition (e.g. Thirlwall et al., 1996). The local
418 sediments are mainly terrigenous, and it was suggested that biogenic (organic-rich) sediments,
419 which typically have more radiogenic Pb, would be necessary to explain the isotopic composition
420 of the Lesser Antilles lavas (Thirlwall et al., 1996). Recently, Carpentier et al. (2008; 2009)
421 presented new isotopic data for local sediments including those from Barbados, DSDP site 543
422 and DSDP site 144. At the latter site, black shales (present only in Unit 3) with extremely
423 radiogenic Pb were encountered (e.g. Carpentier et al., 2008; 2009) and could possibly represent
424 the "missing endmember".

425 We calculated the "minimum" isotopic composition, i.e. the composition with the lowest
426 Sr and Pb isotope ratios and highest Nd and Hf isotope ratios, necessary for any assimilant that
427 would be able to explain Pre-SVC2 and SVC signatures using reasonable parameters. This was

then compared to the composition of the local sediments to assess the most likely relative contribution of terrigenous versus biogenic sediment (such as black shales). We used the AFC equations of De Paolo (1981), in which several parameters must be accounted for: (1) the initial magma composition, (2) the bulk partition coefficient for which the fractionating assemblage and the partition coefficients need to be known, (3) the fraction of melt remaining, "F", , the (4) trace element and isotopic composition of the assimilant and (5) the assimilation / crystallisation ratio or assimilation rate, "r".

As in the least squares models, and for the same reasons, the most mafic Pre-SVC1 lava (SL-83-44) was used for the initial magma composition for trace elements. For the isotopic composition, we again used SL-83-44 (basalt), along with SL-83-25 (basaltic andesite) to encompass most of the range of isotopic compositions observed in the Pre-SVC1 samples. For each element, the bulk partition coefficients were calculated using the assemblages produced by the two best least square models obtained for SVC andesite (models #1 and 2; Table 2) and the compilation of partition coefficients (k_{dS}) presented in Table 3. We ensured that the amount of fractionating assemblage, and therefore the amount of melt remaining, was constant in every isotope-isotope space modelled. The SVC volcanic rocks display some isotopic variation, precluding the modelling of all SVC samples by the same amount of fractionation. In each isotope-isotope space, we used the F value suggested by the least squares models (F~15%; corresponding to ~85% fractionation) for the most extreme lava composition of the SVC (highest Sr and Pb isotope ratios and lowest Nd and Hf isotope ratios). This resulted in all SVC lava compositions being explained with F ranging between ~80% and 15%.

449 Given that reasonable assumptions can be made for the first three factors, we can constrain
450 the trace element composition of the assimilant, its "minimum" isotopic composition (5) and the
451 rate of assimilation (6).

452 *The best fit for trace elements and isotope compositions of the assimilant*

453 As discussed in the previous section, the assimilant displays higher La/Sm and Th concentration
454 than the Pre-SVC1 lavas. Such characteristics can be found in all local sediments that have been
455 analysed (Carpentier et al., 2008), except the Oceanic Formation in Barbados, which contains ash
456 layers. Because the magmas erupting in the southern arc are thought to have intruded through the
457 Aves Ridge forearc basin, any sediments from the Grenada and Tobago basins could represent the
458 assimilant. These two basins accumulated up to 14 km of sedimentation that started in the
459 Paleogene. Sequences deposited before Lesser Antilles magmatism were mainly derived from the
460 South American continent, with only minor amounts from the Aves Ridge (Aitken et al., 2011 and
461 references therein). Because no published trace element compositions exist for the Grenada and
462 Tobago sediments, we used published compositions of the sediments located on the subducting
463 slab near the trench since they were shown to derive dominantly from the Amazon tributary
464 draining the Guyana and Brazilian cratons (Allegre et al., 1996). We investigated different options
465 for trace element concentrations of the assimilant including: (a) the bulk composition of site 144
466 (mainly biogenic), (b) the bulk composition of site 543 sediment (below the décollement found at
467 ~170m in the sequence; mainly terrigenous), (c) the bulk composition of the Scotland Formation
468 of Barbados (terrigenous) and (d) a mix of 50 % each of bulk compositions of sediments from
469 DSDP sites 543 and 144 (reflecting a sequence comprising similar amounts of biogenic and
470 terrigenous sediments; bulk compositions for each site were determined by Carpentier et al. (2008;

2009)). Subsequently, we determined the minimum isotopic composition of the assimilant required to model the Pre-SVC2 and SVC lavas.

Sr, Nd, Hf and Pb concentrations of the assimilant; No good fit was obtained using the bulk trace element composition of sediments from the three different sites (a,b,c); mainly due to Sr/Nd being either too low, or too high suggesting that the assimilant cannot be pure terrigenous or biogenic sediment. However, a 50-50% mix of bulk site 144 and bulk site 543 sediments (d), results in Sr/Nd, Hf/Nd and Nd/Pb (~20, ~0.15, ~1.75, respectively) that can explain the trends observed in the isotope-isotope diagrams (Fig. 4a,b,c,d). This mixed sediment has Sr, Nd, Hf and Pb concentrations of 383 ppm, 22.7 ppm, 2.5 ppm, 13.0 ppm, respectively.

"Minimum" isotopic composition of the assimilant; Taking into account all the previous parameters (See supplementary data file 1 for all parameters and AFC model data), the "minimum" composition permissible for the assimilant is: $^{87}Sr/^{86}Sr$ = 0.7091, $^{143}Nd/^{144}Nd$ = 0.51205, $^{176}Hf/^{177}Hf$ = 0.28227, $^{206}Pb/^{204}Pb$ = 19.81, $^{207}Pb/^{204}Pb$ = 15.85, $^{208}Pb/^{204}Pb$ = 39.54 (Fig. 4a-d). The presence of amphibole (<1%) in the fractionating assemblage results in insignificant changes in the modeled trends on the isotope-isotope diagrams. The use of SL-83-25 as a starting composition results in a better fit than using SL-83-44. This 'minimum' isotopic composition of the assimilant to explain the Pre-SVC2 and SVC volcanic rocks compositions requires a rate of assimilation (r) of ~0.8. This value is considered reasonable since high rates of assimilation ($r \geq 1$) are a feature of recent models (Beard et al., 2005) whereby bulk assimilation of crust is driven by reactions during melting, limiting the energy necessary for the process to proceed. Given that all the parameters used in this model are reasonable, we suggest that the modeled "minimum" composition for the assimilant is realistic.

493 *Best fit for L/M-HREE and Ba/Th versus isotopes models*; Given that the variations in
494 isotopic compositions of St Lucia volcanic rocks are correlated with variations in REE patterns
495 and LILE/HFSE, we verified that the 50-50% mix of bulk site 144 and bulk site 543 sediments,
496 having ideal Sr, Nd, Hf and Pb concentrations to model the isotopic variations, also had suitable
497 REE and Ba, Th and U concentrations to explain the high La/Yb and La/Sm (Fig. 4e,f) and the
498 observed Ba/Th and Th/Th* of the volcanic rocks using the same model parameters. This mixed
499 sediment has La, Sm and Yb concentrations of 25.16 ppm, 4.48 ppm and 1.90 ppm, with La/Sm
500 and La/Yb of 5.6 and 13.2 and Ba and Th concentrations of 562 ppm and 7.8 ppm, respectively.

501 The increase in La/Yb and La/Sm observed from Pre-SVC1 to Pre-SVC2 lavas are very
502 well reproduced by the model with no change in parameters. The La/Yb and La/Sm ratios of SVC
503 volcanic rocks can also be modeled very well. However, more residual melt (and therefore less
504 mineral fractionation) than the amount determined by the least squares models is needed to explain
505 the SVC andesite compositions (F ~15%). This can be observed in Fig. 4e and f which shows that
506 using both amphibole-bearing and amphibole-free assemblages, the La/Yb composition of the
507 SVC andesites plot between F = 70-55 % which corresponds to 30-45% fractionation, and the SVC
508 andesites La/Sm plot between F = 70-20 % (F =70-55 % for amphibole-bearing assemblage and F
509 = 55-20 % for the amphibole-free assemblage).

510 This F discrepancy could be argued to be due to the use of La/Sm and La/Yb assimilant
511 values that are too high. However, a decrease of these ratios to unreasonable values (La/Yb = 5.3;
512 La/Sm ≤ 4.24) would be necessary in order to model the SVC andesites compositions with F ~ 15
513 %. Indeed, no local sediment would have low enough La/Yb and La/Sm while having $^{87}Sr/^{86}Sr$
514 radiogenic enough (Fig. 4e) to explain the andesite compositions. Therefore, we suggest that the
515 F discrepancy in the L/M-HREE versus isotope ratio model may result from the interplay of both

(1) values of La/Sm and La/Yb that are slightly too high in the assimilant used and (2) an overestimation of the amount of fractionation obtained by the major element least squares models which may instead be comprised between 55 and 75% (F = 45-25 %). The overestimation of the amount of fractionation could easily be explained by the fact that the system is open, and may be caused by the impact of both recharge events and assimilation on the major element composition of the SVC magmas. In addition, the overestimate could also result from the use of an invariant fractionated mineral assemblage in the AFC model. The impact of this potential overestimation of F on the modeled "minimum" assimilant composition from the isotope data is nevertheless insignificant. Indeed, using F ~ 55 % instead of F ~ 15 % to model the most extreme SVC signature in the isotope-isotope models yields a very similar minimum assimilant isotopic composition: $^{87}Sr/^{86}Sr=0.7093$, $^{143}Nd/^{144}Nd=0.5120$, $^{176}Hf/^{177}Hf=0.28220$, $^{206}Pb/^{204}Pb=19.83$, $^{207}Pb/^{204}Pb=15.85$, $^{208}Pb/^{204}Pb=39.54$ (see supplementary file 1).

In a similar way to La/Sm and La/Yb, the SVC Ba/Th were modeled successfully, but with F > 20 % (Fig. 4g) which supports the inference of an overestimation of fractionation from the REE. However, unlike the REE, the choice of a sediment with slightly higher Ba/Th compared to the composition of the mix used is possible and could cancel the small F discrepancy. A sediment with a slightly higher Ba/Th (~83 instead of 72 for the mix) would be consistent with the Th/Th* necessary to model the composition of Pre-SVC2 and SVC volcanic rocks. Indeed, using the Ba, Th and U content of the 50-50% mix of bulk site 144 and bulk site 543 sediments manages to successfully reproduce the Th/Th* increase between Pre-SVC1 and SVC, as shown in Fig. 5g. However, for the model path to go through Pre-SVC2 lavas, the sediment assimilated needs to have a slightly lower Th/Th* (0.93) than the mix of 50% bulk site 543 + 50% bulk site 144 sediment used (1.07; Fig. 5g).

539 *Comparison of the "minimum" assimilant composition with the local sediments*

540 The modeled isotopic composition of the assimilant overlaps Units 1 and 2 of DSDP site 144
541 sediments in terms of Sr, Nd and Pb isotopes but is also not very different from site 543 and
542 Barbados sediment compositions (Fig. 4). In terms of Hf isotope ratio, the assimilant plots amongst
543 the less radiogenic compositions of Barbados and Unit 1 and 2 of site 144 sediments. Black shales
544 such as those present in Unit 3 of DSDP site 144, and which display the most radiogenic Pb
545 isotopic composition known in the Caribbean area, are not required in the St Lucia basement to
546 explain SVC lava isotopic compositions. In fact, although our modeled assimilant represents the
547 "minimum" composition which means the assimilant could be more radiogenic, assimilation of
548 black shales seems very unlikely. This is because black shales all display $^{206}Pb/^{204}Pb > 21$ which
549 can hardly be reached by a model that goes through the SVC volcanic rock compositions. It is
550 particularly obvious on the $^{143}Nd/^{144}Nd$ vs. $^{206}Pb/^{204}Pb$ diagram (Fig. 4d). Furthermore, the black
551 shales have higher $^{176}Hf/^{177}Hf$ than some SVC lavas (>0.2824), which argues against their
552 likelihood of representing the assimilant. Carbonate-rich sediment similar to Units 1 and 2 of site
553 144 could fit with the isotopic composition of our assimilant. However, as mentioned earlier, these
554 sediments have a mean CaO of ~30 wt. % and significant plagioclase and/or clinopyroxene
555 fractionation would be needed to offset the related CaO increase in the magma during assimilation.
556 Furthermore, the trace element composition of such sediments is not suitable because the Sr/Nd is
557 too high (Mean Units 1 and 2 sediment Sr/Nd = 62 while Sr/Nd needed in the model is ~20).
558 Terrigenous sediments from DSDP 543 and Barbados have isotopic compositions very close to
559 the modelled assimilant. However, like site 144 Unit 1-2 sediments, their trace element
560 composition is not suitable for modelling St Lucia volcanic rocks because Sr/Nd (~4) is too low.
561 We therefore suggest that the assimilant is more likely to be a mix of terrigenous and biogenic

562 sediment, since this would fulfil all the characteristics of the assimilant, both in terms of major,
563 trace elements and isotopes. Such an interpretation would be in agreement with the heterogeneous
564 composition of the sequences found in the Grenada and Tobago basins, through which the arc
565 magmas are thought to have intruded. Indeed the basin sequences comprise deep-water turbidite,
566 pelagic and volcanogenic shales and siltstone, with some biogenic limestone in the deeper parts
567 (Aitken et al., 2011).

568 **THE COMPOSITION OF THE MANTLE SOURCE REGION BENEATH ST LUCIA**

569 Due to the continental signature of the lavas, the mantle source under the south of the arc has long
570 been suspected to comprise more sediment than in the north of the arc and/or sediment with more
571 "continental" isotopic composition (White & Dupré, 1986; Carpentier et al., 2008). However,
572 Bezard et al. (2014) showed that in St Lucia, volcanic rocks with Sr, Nd and Pb isotopic
573 compositions more continental than those of "typical oceanic arc" are in fact the result of
574 assimilation of continent-derived sediment. So are the Hf isotopic compositions and LILE/HFSE
575 and L/M-HREE, as demonstrated in the previous sections. Therefore, based on trace elements and
576 the Sr, Nd, Hf and Pb isotope composition of the lavas which have not been affected by sediment
577 assimilation (i.e. Pre-SVC1 lavas), the source beneath St Lucia may be similar to that beneath the
578 northern islands. However, Bezard et al. (2015) show that, even the composition of lavas that
579 avoided sediment assimilation need to be interpreted with care. Indeed, some lithophile isotopic
580 and trace element features of some of the most primitive lavas along the arc (including Pre-SVC1
581 lavas) were shown to result from assimilation of igneous basement early during magma
582 differentiation (Bezard et al., 2015). Below, using all these constraints, we interpret St Lucia source
583 characteristics and compare these with the rest of the arc.

584 **Crustal assimilation by Pre-SVC1 magmas?**

585 The absence of a correlation between SiO_2 and radiogenic isotopes (Fig. 5a, b, c, d), Ba/Th (not
586 shown) and L/M-HREE (Fig. 5e) in the Pre-SVC1 lava compositions suggest that their magmas
587 avoided substantial sediment assimilation during differentiation from basalt to rhyolite, and could
588 therefore have preserved St Lucia mantle source characteristics. However, their low MgO values,
589 even for the most mafic lavas of this suite, indicates that they evolved from a more primitive
590 precursor. Therefore, the possibility of cryptic assimilation, either during basaltic differentiation
591 from the primary magma and/or between basalt and rhyolite differentiation, needs be considered.

592 Methods to investigate assimilation of crust during the production of Pre-SVC1 basalt are
593 limited. Bezard et al. (2014) shown that $\delta^{18}O$ values of pyroxene and plagioclase phenocrysts from
594 Pre-SVC1 basalt lie at the upper-end of, or slightly above their mantle ranges. This suggests that
595 these crystals grew in a magma that assimilated very limited amounts of sediment (having high
596 $\delta^{18}O$). Such limited amounts are unlikely to have had substantial effects on the whole rock isotopic
597 composition (Bezard et al., 2014). On the other hand, assimilation of an igneous component with
598 mantle-like $\delta^{18}O$ by the primary magmas, leading to Pre-SVC1 basalt compositions, cannot be
599 precluded and has been recently suggested by Bezard et al. (2015). These authors used Os isotope
600 data to show that, except for Grenada, the most primitive lavas found along the arc, including Pre-
601 SVC1 basalt SL-83-44, were affected by assimilation of plagioclase-rich cumulates in the deep arc
602 crust. This is suggested to decrease $^{87}Sr/^{86}Sr$ and La/Sm and increases Sr/Th in the primary magmas
603 while keeping unmodified $\delta^{18}O$, Nd isotopes and Pb isotopes (Bezard et al., 2015).

604 Assimilation of igneous crust may also explain some or all the compositional variations
605 observed amongst Pre-SVC1 samples. While Pre-SVC1 $^{143}Nd/^{144}Nd$ and $^{207}Pb/^{204}Pb$ isotope
606 compositions are nearly identical, some small variations are observed for $^{87}Sr/^{86}Sr$, $^{176}Hf/^{177}Hf$,

607 $^{208}Pb/^{204}Pb$ and $^{206}Pb/^{204}Pb$ (Fig. 4). These variations do not follow the same trajectory as the SVC
608 and Pre-SVC2 AFC trend, and cannot be explained by assimilation of any local sediments. Instead,
609 they could either be explained by variations in the composition of the mantle source (either pre-
610 existing variations in the mantle wedge or variations in the composition of the subducted sediment)
611 or by variable amount of assimilation of igneous crust. Once again, discriminating between source
612 and crustal processes using lithophile radiogenic isotopes and the mineral $\delta^{18}O$ data available is
613 not straightforward. Indeed, the overlap of mineral $\delta^{18}O$ with the mantle range, the very limited
614 radiogenic isotope variation in Pre-SVC1 group and the absence of correlations between these
615 indices and SiO_2 do not preclude sporadic assimilation, or assimilation of material with SiO_2 and
616 $\delta^{18}O$ compositions resembling that of the magma. As mentioned above, $^{187}Os/^{188}Os$ was shown to
617 be a powerful tool to detect assimilation of igneous material but was analysed in only one basalt
618 from St Lucia. Given that plagioclase-rich cumulate assimilation likely modified the composition
619 of the primitive magma, it could also be responsible for some of the small compositional variations
620 observed amongst Pre-SVC1 lavas. However, assimilation of plagioclase cumulates was shown to
621 only clearly affect Sr isotopes, hence, variations of at least Nd and Pb isotopes and maybe Hf
622 isotopes (which were not investigated by Bezard et al. (2015) since no data were available for most
623 of the lavas analysed) need to be explained by either another assimilant or a source process.
624 However, in the absence of evidence for the former hypothesis, a source origin is the most plausible
625 explanation for the isotopic variations observed.

626 **Amount of subducted sediment in the source**

627 Given that part of the composition of the most primitive lava of the island is likely affected
628 by cumulate assimilation and that the small isotopic variations observed amongst Pre-SVC1 lavas
629 may also be due to assimilation, constraining the source characteristics of the primitive St Lucia

magmas, such as the amount and the isotopic composition of slab-derived material added to the mantle, is not straightforward. However, the maximum amount of sediment involved in the mantle source can be estimated using mixing models and published compositions of the subducting slab units.

Slab components in the magma source region could be inherited from (1) fluids or melts from the subducting sediments and/or (2) fluids or melts from the subducted basaltic oceanic crust. White et al. (1985) found that the isotopic composition of DSDP site 543 basalt, on the subducting plate had a typical MORB composition ($^{87}Sr/^{86}Sr$ = 0.7030-0.7033; $^{143}Nd/^{144}Nd$ = 0.513048-0.513084; $^{206}Pb/^{204}Pb$ = 18.437-18.470; $^{207}Pb/^{204}Pb$ = 15.54-15.57 $^{208}Pb/^{204}Pb$ = 38.03-38.11). This means that fluids/melts derived from basalt dehydration/melting should have a negligible impact upon the Sr, Nd, Hf and Pb isotopic compositions of the mantle wedge. Hence, only the subducted sediments would possibly affect the mantle isotopic signature. Given the very restricted composition of the Pre-SVC1 lavas, our only option to determine the maximum amount of sediment involved is to use the "least continental" isotopic composition of the local sediment and their trace element compositions, in a mixing model passing through the mean Sr, Nd, Hf and Pb Pre-SVC1 lavas composition using the depleted mantle (Workman & Hart (2005) for trace element and White et al. (1985) for isotopic compositions) as a starting composition. In addition, we repeated the models using the $^{87}Sr/^{86}Sr$ of Grenada's most primitive picrite for Pre-SVC1 lavas since plagioclase cumulate assimilation has been suggested to reduce the $^{87}Sr/^{86}Sr$ of St Lucia primitive magma from values similar to Grenada picrite to that observed in Pre-SVC1 basalt (Bezard et al., 2015). This allows the evaluation of the influence plagioclase cumulate assimilation on the maximum amount of sediments obtained by the models.

652 Three local sedimentary sequences that represent possible subducted sediments are: the
653 DSDP site 543 sediments, site 144 sediments and sediments similar to those preserved on Barbados
654 (although the latter was accreted, it cannot be ruled out that similar sediment could also have been
655 subducted). These three sedimentary sequences not only display large ranges in Sr-Nd-Hf-Pb
656 isotope composition, they also display large differences in trace element concentrations and ratios
657 (Carpentier et al., 2008; 2009). The greatest difference is seen in very high Sr and low Nd, Hf and
658 Pb concentrations in site 144 sediments compared to site 543 and Barbados. Such high Sr produces
659 Sr/Nd, Sr/Hf and Sr/Pb ratios up to 15 times higher than at site 543 and Barbados, while there are
660 insignificant differences in Nd/Hf, Nd/Pb and Hf/Pb between all three sets of sediments. Because
661 elemental concentrations and ratios strongly influence the shape of mixing curves, we performed
662 models using extreme concentrations and elemental ratios to encompass the whole range of bulk
663 local sediment composition variations. Elemental ratios of the sediment component are also very
664 dependent on whether it is incorporated as a solid ('bulk'), or is incorporated through fluids or
665 partial melts in the mantle. Therefore, we subsequently discuss the differences in the amount of
666 sedimentary component required in the mantle to model Pre-SVC1 lava compositions in the case
667 of fluids and melts incorporation.

668 In the first model, we used the trace element composition of the bulk site 144 (B144)
669 sediments, which have the highest Sr concentrations and the highest Sr/Nd with the lowest Pb
670 concentration and a low Pb/Hf (3.4) similar to the lowest bulk value corresponding to Barbados
671 (2.7). In the second model we used the trace element compositions of the bulk site 543 (B543)
672 sediments which have the lowest Sr concentration and Sr/Th and the highest Pb and Pb/Hf ratios
673 (6.7). Bulk sediment concentrations at each DSDP site were used to represent the average of the
674 whole subducting pile. We present the models in both the $^{87}Sr/^{86}Sr$-$^{143}Nd/^{144}Nd$ and the

675 $^{176}Hf/^{177}Hf$-$^{207}Pb/^{204}Pb$ diagrams (Fig. 7) in which we fixed the highest realistic Nd and Hf isotope
676 compositions of the local sediment to $^{143}Nd/^{144}Nd = 0.5122$ and $^{176}Hf/^{177}Hf = 0.2827$. These values
677 correspond to the highest Nd and Hf isotope composition amongst the local sediment having
678 similar to or more radiogenic Sr and Pb isotopic compositions than the lavas (Barbados sediment
679 containing ash layers, are not considered since they are at the top of the sedimentary sequence and
680 are unlikely to have been subducted). Models 1 and 2 were constrained to pass through the mean
681 composition of the Pre-SVC1 lavas and the Sr and Pb isotopic compositions of the sediment end-
682 member was constrained to realistic isotopic compositions, i.e. plotting in the compositional field
683 of the local sediments. The position of Pre-SVC1 samples on the two modeled curves of each
684 diagram constrains the maximum amount of sediment involved in the source of the lavas for the
685 whole spectrum of Sr and Pb concentrations and Sr/Nd and Pb/Hf of the local sediments at these
686 fixed Nd and Hf isotopic composition. Decreasing $^{143}Nd/^{144}Nd$ and $^{176}Hf/^{177}Hf$ of the sediment
687 used in the model toward more "continental" compositions, while still permitting the model to pass
688 through Pre-SVC1 lava compositions, will decrease the amount of sediment necessary to explain
689 Pre-SVC compositions. Hence, we can be confident that our models constrain the maximum
690 possible amount of bulk local sediment in the source, if $^{87}Sr/^{86}Sr$ of the Pre-SVC1 lavas represent
691 the primary magma composition. We also produced Models 1' and 2' passing through potential
692 lava compositions characterized by $^{87}Sr/^{86}Sr$ of Grenada picrite but $^{143}Nd/^{144}Nd$ of Pre-SVC1 lavas
693 (Pre-SVC1') to constrain the maximum possible amount of bulk local sediments in the source, in
694 a case where plagioclase cumulate assimilation affected the $^{87}Sr/^{86}Sr$, as suggested by Bezard et
695 al. (2015). To do so, the minimum $^{87}Sr/^{86}Sr$ of the subducted sediment for Model 1' was increased
696 compared to model 1 (from 0.7066 to 0.7087). For Model 2', given that no subducting sediment
697 can possibly have higher $^{87}Sr/^{86}Sr$ than that used in Model 2, the only option to make a model go

698 through the Pre-SVC1' compositions was to increase the Sr content of the sediment in the source
699 (from 110 to 184 ppm).

700 The best fit obtained using B144 Sr and Nd concentrations, in both Models 1 and 1',
701 involves between 0.6-0.8% of bulk sediment in the mantle source of Pre-SVC1 lavas; using site
702 543 sediment composition (Model 2) or similar (Model 2') requires 0.2-0.4% of bulk sediment in
703 the source. Using Hf and Pb concentrations from either B144 or B543 implicates between 1 and
704 2% of sediments in the source (the higher "maximum" value obtained using Pb/Hf compared to
705 Sr/Nd is due to the smaller isotopic difference between the least "continental" local sediments and
706 the DMM). Therefore, even taking into account the large variations in trace element composition
707 of the local sediments, and potential decrease of $^{87}Sr/^{86}Sr$ by cumulate assimilation, the amount of
708 bulk sediment needed in the source does not exceed 2%. Such a low amount of sediment in the
709 mantle wedge source is similar to amounts estimated for the north of the arc (~2% by Turner et
710 al., (1996); 1% by Carpentier et al. (2008); <1% by Davidson & Wilson (2011) for Statia), as well
711 as for Martinique (<1%; Davidson & Wilson, 2011), Grenada (0.2-2%; Thirlwall et al., 1996) and
712 the whole arc (0.2-2% bulk sediment addition for the Lesser Antilles source by DuFrane et al.
713 (2009)).

714 The models discussed above involve incorporation of bulk sediments in the mantle.
715 However, depending on the slab conditions, sediment could be introduced as partial melts or fluids,
716 rather than bulk sediments, (DuFrane et al., 2009; Labanieh et al., 2012). Sr/Nd and Pb/Hf are
717 different in sediment melts and in sediment fluids compared to the bulk sediments, due to the
718 presence of residual phases during melting and different mobility of these elements in aqueous
719 fluids respectively. Discrimination between the addition of bulk sediment, sediment fluid or
720 sediment melt to the mantle source is not straightforward. Sr/Th, U/Th and Ba/Th (i.e.

721 LILE/HFSE) are often used to detect the influence of slab-derived fluids in the lava mantle source
722 since Sr, U and Ba are preferentially incorporated into the fluid phase (e.g. Johnson & Plank, 1999)
723 while Th is not and can only be added as bulk sediment or sediment melt to the mantle (e.g.
724 Hawkesworth et al., 1997; Plank, 2005). In Pre-SVC1 no correlation exist between LILE/HFSE
725 (e.g. Sr/Th, U/Th and Ba/Th) and Sr or Pb isotopes which suggests that if slab derived fluids are
726 responsible for the variations observed in LILE/HFSE, they cannot come from the dehydration of
727 the subducted sediments. Indeed the latter have very continental signatures and would produce a
728 positive correlation between LILE/HFSE and Sr or Pb isotopes. Instead, the LILE/HFSE variations
729 would need to come from the dehydration of the mafic and/or ultramafic parts of the subducing
730 slab, which would have an isotopic composition similar to MORBs. Therefore, although it cannot
731 be precluded that a correlation between Sr isotopes and LILE/HFSE, might be masked by
732 assimilation of igneous basement (Bezard et al., 2015), the absence of correlation between
733 LILE/HFSE and Nd, Hf and Pb isotopes suggest that the displacement to more 'continental'
734 isotopic compositions of Pre-SVC1 lavas isotopic signatures compared to MORBs is not produced
735 by slab-derived fluids, but instead by sediment or sediment melt.

736 La/Sm ratios have been used in conjunction with Nd or Hf isotopes by some authors to
737 discriminate between sediment and sediment melt addition to the mantle, based on the comparison
738 of the lava compositional trend with the mixing lines produced by incorporation of sediment and
739 sediment melts to the depleted mantle (e.g. Labanieh et al., 2012). However the La/Sm
740 compositions of Pre-SVC1 lavas are close to those of the depleted mantle and overlap fresh
741 Atlantic MORB compositions (not shown). Therefore, they cannot be used to discriminate between
742 melt and bulk sediment input in the mantle. The possible occurrence of sediment melt in the St
743 Lucia mantle source could be deduced from the conditions of the slab (P, T°). These conditions

744 could, in turn, be determined by detecting the presence of certain accessory slab minerals, using
745 the isotopic and trace element signatures of the lavas. For example, key ratios such as Zr/Hf (e.g.
746 Hermann and Rubatto, 2009) or the decoupling of Hf and Nd isotopes can be used to detect the
747 presence of residual zircon in the slab. However, in St Lucia, the absence of clear trends in the
748 Pre-SVC1 lavas renders the detection of residual zircon, and therefore, the determination of the
749 slab conditions impossible. Similarly, detection of rutile and amphibole residual phases (and
750 discrimination of their relative impact) using Nb/Ta vs Zr/Sm (Konig and Schuth, 2011) is not
751 possible since Pre-SVC1 lavas do not show any trend and plot within the MORB range.

752 In the absence of clear evidence for the nature of the sediment component and to account for all
753 scenarios (even the case where sediment components are added by fluids), we calculated the melt
754 Sr/Nd and Pb/Hf as well as the fluid Sr/Nd of B144 and B543 sediments (fluid Pb/Hf could not be
755 calculated since the Hf partition coefficient is not available) using partition coefficients from
756 Johnson & Plank (1999) and Hermann & Rubatto (2009) (see Supplementary data file 1). Results
757 show that, compared to the bulk sediment, both melts and fluids display higher Sr/Nd (Melts: 18.21
758 for B543 melt and 224.51 for B144; fluids: 17.49 for B543 and 215.61 for B144) and that melts
759 also have higher Pb/Hf (20.76 for B543melt and 10.43 for B144 melt). These higher ratios require
760 slightly more sediment melt or fluids in the mantle source to explain Pre-SVC1 lavas, compared
761 to bulk sediments. Indeed using Sr and Nd concentrations, for both sites 144 and 543, the amount
762 of sediment melt needed to explain Pre-SVC1 lava compositions ranges between 1 and 3% and
763 the amount of sediment fluid needed ranges between 0.8 and 3% Using Hf and Pb concentrations,
764 between 2 and 3.5% of sediment melt are needed in the mantle source. Therefore, a maximum of
765 3.5% sediment melt or 3% sediment fluids can be invoked to explain both the Sr-Nd and Pb-Hf
766 isotopic composition of Pre-SVC1 lava source. As for the models involving bulk sediments, these

767 percentages represent maximum values. Indeed, most site 543 and 144 sediments have lower
768 $^{176}Hf/^{177}Hf$ (bulk sites 543 and 144: 0.28256 and 0.28236 respectively; Carpentier et al., 2009) and
769 $^{143}Nd/^{144}Nd$ values (bulk sites 543 and 144: 0.511966 and 0.512014 respectively; Carpentier et al.,
770 2009) than those used in the model. Nevertheless, the involvement of 3.5% sedimentary
771 component in the mantle source would still be much lower than some values obtained without
772 taking sediment assimilation into account (e.g. 10% sediments in Carpentier et al., 2008).

773 **Comparison of the St Lucia source composition with the rest of the arc**

774 Although small amounts of plagioclase cumulate assimilation may have affected Pre-SVC1 lavas,
775 these represent the lavas with the composition closest to that of the source beneath St Lucia.
776 Keeping in mind the effect of cumulate assimilation, we now compare their inferred mantle source
777 characteristics with the potential source beneath the other islands.

778 In order to compare St Lucia source (Pre-SVC1) compositions with the rest of the arc, we
779 plotted, on Fig. 8, combinations of the most commonly used isotopic and trace element proxies for
780 all Lesser Antilles samples available in the literature: $^{87}Sr/^{86}Sr$, $^{143}Nd/^{144}Nd$ and $^{206}Pb/^{204}Pb$ against
781 MgO, La/Sm and Ba/Th ($^{176}Hf/^{177}Hf$ was not plotted as very few data are available). In addition,
782 we selected the most mafic lava composition available from each island and plotted them on Figs.
783 7 and 9.

784 *St Lucia and the north of the arc*

785 Based on the composition of the most mafic lavas, the mantle source beneath the northern
786 islands would have similar La/Sm, Ba/Th, $^{143}Nd/^{144}Nd$ (except for Dominica), but slightly less
787 radiogenic $^{87}Sr/^{86}Sr$ and less radiogenic $^{206,207,208}Pb/^{204}Pb$ than that inferred for St Lucia (Fig. 8, 9).
788 The similar range of Ba/Th argues for a similar fluid/sediment ratio beneath the northern islands

and St Lucia. The similar Nd isotopic composition could also be consistent with a similar amount of sediment in the source. Their similar La/Sm could indicate that the sediment composition and the process of incorporation into the source (melt vs bulk sediment) do not change substantially from north to south, but this ratio is likely buffered by cumulate assimilation (Bezard et al., 2015) and should therefore not be used as a source indicator. Similarly the higher $^{87}Sr/^{86}Sr$ of Pre-SVC1 lavas compared to the northern islands might be due lower amounts of plagioclase cumulate assimilation. On the other hand, Pb isotopes were not shown to be affected by the latter process, and the higher Pb isotope ratios of St Lucia Pre-SVC1 lavas compared to the northern lavas could be explained by sediment with more radiogenic Pb in the mantle source of St Lucia. We prefer this to the alternative argument that the more radiogenic Pb isotope ratios of Pre-SVC1 lavas compared to the northern islands were produced by very small amounts of sediment assimilation, where only Pb isotopes were sensitive to assimilation, due to larger differences in concentration of these elements between the magma and the assimilant than for Nd. While this would be consistent with the Pre-SVC1 mineral $\delta^{18}O$ data plotting close to the upper end of the mantle range, it is not supported by the small differences in Pb and Nd concentrations observed between Pre-SVC1 basalt and the inferred composition of the assimilated sediment. Indeed, the modeled sediment assimilated (similar to 50-50% mix of site 144 and site 543) has ~3.2 times more Nd than Pre-SVC1 basalt which is not much lower than the ratio for Pb (~5 times). Yet, we do not observe a displacement of Pre-SVC1 $^{143}Nd/^{144}Nd$ compared to the northern islands, anticipated for assimilation of sediment able to increase Pb isotopes. Therefore, we suggest that the Pb isotopic contrast between St Lucia (Pre-SVC1) and the northern islands are not due to subtle sediment assimilation. Instead, we explain these by the more radiogenic nature of the subducted sediment present in the mantle beneath St Lucia.

St Lucia and the south of the arc

Compared to the northern islands, variations in the isotopic and trace element compositions of the southern lavas are important (Fig. 8a, b, c). However, the largest variations are found in the most differentiated rocks (typically in lavas with MgO below 5 wt. %) which comprise both compositions overlapping the northern arc and very 'continental' signatures, while the most mafic lavas only present limited heterogeneities. The absence of important compositional changes in the most mafic lavas suggests the variations observed in the southern islands could be mostly produced during magma differentiation. Furthermore, lavas from Martinique (Labanieh et al., 2010; 2012), Grenada (Thirlwall et al., 1996) and Bequia (Smith et al., 1996), which display the largest heterogeneities and the most 'continental' signatures (along with St Lucia), display co-variation of Sr, Nd, Hf, Pb isotopes, Ba/Th and of La/Sm, like in St Lucia (Fig. 8a, b, c). This strongly argues for the production of compositional heterogeneities, and therefore the production of the continental signatures observed, by assimilation of a similar sediment to that inferred for St Lucia. Hence, like in St Lucia, it is critical to use the most mafic lavas available to investigate the source of the southern island lavas.

The most mafic lavas of Bequia, St Vincent and Martinique have La/Sm, Ba/Th, $^{87}Sr/^{86}Sr$ and $^{143}Nd/^{144}Nd$ overlapping the Pre-SVC1 and northern islands range. They have Pb isotope signatures increasing from compositions similar to the northern islands (in Martinique and St Vincent) to compositions clearly higher than those of the Northern islands and St Lucia (in Bequia; Fig. 8, 11). Primitive lavas from Grenada, Ile de Caille and Kick'em Jenny have variable La/Sm and some of the lowest Ba/Th and $^{143}Nd/^{144}Nd$ in the arc, although these ratios still overlap the range observed in the northern islands. They are, however, clearly distinguished from the rest of the arc by their higher Sr and Pb isotopes composition. Although the involvement of larger

amounts of sediment cannot be ruled out, the overlap of $^{143}Nd/^{144}Nd$ and Ba/Th with the range observed in the north of the arc suggests that the more radiogenic Pb isotopes signatures of the lavas more likely reflect the more radiogenic nature of sediment introduced in the mantle source.

In summary, based on overlapping Ba/Th and $^{143}Nd/^{144}Nd$ of the most mafic lavas, no major contrast in slab-derived fluid /sediment ratio can be observed between the sources of the southern and the northern arc, except maybe for Grenada, Ile de Caille and Kick'em Jenny. The along arc variations in Pb and Nd isotopic signatures amongst mafic lavas most likely reflect different isotope compositions of the sediment in the source. The variations in La/Sm and $^{87}Sr/^{86}Sr$ could also result from variable sediment composition in the source, but have also been suggested to result from cumulate assimilation (Bezard et al., 2015). The presence of sediment with more radiogenic Pb in the source of the southern islands compared to the north of the arc has been suggested in the past (e.g. Carpentier et al., 2008). However, previous estimates of the nature and composition of these sediments were made using the whole Lesser Antilles arc lava dataset, without taking into account the degree of differentiation of the lavas, especially crustal assimilation. Here we show that isotopic variations in the most mafic lavas are restricted compared to the variations observed when lavas of all degrees of differentiation are selected. Therefore, previous estimates of the nature and isotopic composition of the subducted sediments, based on the whole Lesser Antilles arc lavas dataset, are biased and need to be reassessed. These studies include that of Carpentier et al. (2008) who suggested the need for 10% of subducted sediment with extreme Pb isotopic compositions such as those found in site 144 sediments, to explain the southern islands lava compositions.

CONCLUSIONS

Volcanic rocks with continental isotopic compositions observed in St Lucia are produced by high rates of assimilation of sediment in the arc crust, which are responsible for the co-variation of Sr, Nd, Hf and Pb isotope ratios, L/M-HREE and Th/Th* with SiO_2. The sediment assimilated is likely to be a mix of biogenic and terrigenous sediments originating from the South American continent. Some lavas escaped significant sediment assimilation, these have signatures close to "typical oceanic arc" isotopic signatures with similar Ba/Th, La/Sm, Nd isotope ratios to the northern island mafic lavas but slightly more radiogenic Sr and Pb isotopes. Such lavas can be produced by the addition of less than 2% of bulk sediment or less than 3.5% of sediment melt or fluid, with more radiogenic Pb than the sediments involved in the mantle source of the northern islands. A comparison of St Lucia with other islands from the south of the arc suggests that the source of Martinique, St Vincent and Bequia magmas is similar to St Lucia. Only Grenada, Ile de Caille and Kick'em Jenny could have a source containing larger amounts of, or more radiogenic sediment. Martinique and Grenada, which along with St Lucia are the two other islands with extreme isotopic compositions, display a similar co-variation of Sr, Nd, Hf and Pb isotope ratios, Ba/Th and L/M-HREE to that observed in St Lucia lavas affected by sediment assimilation. We suggest that assimilation is the only process responsible for the extreme isotopic compositions observed in the arc and that, except maybe for Grenada, Ile de Caille and maybe Kick'em Jenny, the amount of sediment present in the source of the north and the south of the arc is similar. The more radiogenic Pb signatures observed in the southern lavas are instead explained by a more radiogenic sediment.

ACKNOWLEDGEMENTS

Financial support was provided to Rachel Bezard by Durham and Macquarie University cotutelle studentship (No. 2012060). We are grateful to Chris Ottley, Geoff Nowell and Peter Wieland for their assistance during the analytical work. We thank Brian M. Dreyer, Alan Hastie and two

anonymous reviewers for their very constructive comments and Richard C. Price for the editorial handling of the manuscript.

SUPPLEMENTARY DATA

Supplementary data for this paper are available at *Journal of Petrology* online.

REFERENCES

Agner-Torres, M., Blundy, J., Ulmer, P. & Pettke, T. (2007). Laser Ablation ICPMS study of trace element partitioning between plagioclase and basaltic metls: an experimental approach. Contributions to Mineralogy and Petrology 153, 647-667.

Aitken, T., Mann, P., Escalona, A. & Christeson, G.L. (2011). Evolution of the Grenada and Tobago Basins and implications for arc migration. Marine and Petroleum Geology 28, 235-258.

Allègre, C.J., Dupré, B., Négrel, P. & Gaillardet, J. (1996). Sr–Nd–Pb isotope systematics in Amazon and Congo River systems: Constraints about erosion processes. Chemical Geology 131, 93-112.

Aquater, SpA. (1982). Exploration of St. Lucia's Geothermal Resources, Annex A-Geological Survey. The Government of St. Lucia Ministry of Finance and Planning.

Arth, J.G. (1976). Behaviour of trace elements during magmatic processes-a summary of theoretical models and their applications. Journal of Research US Geological Survey 4, 41-47.

Beard, J.S., Ragland, P.C. & Crawford, M.L. (2005). Reactive bulk assimilation: A model for crust-mantle mixing in silicic magmas. Geology 3, 681-684.

899 Bezard, R., Davidson, J.P., Turner, S., Macpherson, C.G., Lindsay, J.M. & Boyce, A.J. (2014).
900 Assimilation of sediments embedded in the oceanic arc crust: myth or reality? Earth and Planetary
901 Science Letters 395, 51-60.

902 Bouysse, P. & Westercamp, D. (1990). Subduction of Atlantic aseismic ridges and Late Cenozoic
903 evolution of the Lesser Antilles island-arc. Tectonophysics 175, 349-390.

904 Briden, J.C., Rex, D.C., Faller, A.M. & Tomblin, J.F. (1979). K-Ar geochronology and
905 paleomagnetism of volcanic rocks in the Lesser Antilles island arc. Philosophical Transactions of
906 the Royal Society of London A291, 485-528.

907 Burke, K. (1988). Tectonic evolution of the Caribbean. Annual Review of Earth Planetary Science
908 Letters 16, 201-230.

909 Carpentier, M., Chauvel, C. & Mattielli, N. (2008). Pb-Nd isotopic constraints on sedimentary
910 input into the Lesser Antilles arc system. Earth and Planetary Science Letters 272, 199-211.

911 Carpentier, M., Chauvel, C., Maury, R.C. & Mattielli, N. (2009). The 'Zircon effect' as recorded
912 by the chemical and Hf isotopic composition of Lesser Antilles forearc sediments. Earth and
913 Planetary Science Letters 287, 86-99.

914 Davidson, J.P. (1984). Petrogenesis of Lesser Antilles island arc magmas: Isotopic and
915 geochemical constraints. PhD thesis, University of Leeds, 308 pp.

916
917 Davidson, J.P. (1987). Crustal contamination versus subduction zone enrichment: example from
918 the Lesser Antilles and implications for mantle source compositions of island arc volcanic rocks.
919 Geochimica Cosmochimica Acta 51, 2185-2198.

920 Davidson, J.P. & Arculus, R.J. (2006). The significance of Phanerozoic arc magmatism in
921 generating continental crust. In: Brown, M & Rushmer, T. (eds) Evolution and Differentiation of
922 the Continetnal Crust. Cambridge: Cambridge University Press, pp. 135-172.

923 Davidson, J.P. & Harmon, R.S. (1989). Oxygen isotope constraints on the petrogenesis of volcanic
924 arc magmas from Martinique, Lesser Antilles. Earth and Planetary Science Letters 95, 255-270.

925 Davidson, J.P. & Wilson, M. (2011). Differentiation and Source Processes at Mt Pelée and the
926 Quill; Active Volcanoes in the Lesser Antilles Arc. Journal of petrology 52, 1493-1531.

927 Davidson, J., Turner, S., Handley, H., Macpherson, C. & Dosseto, A. (2007). Amphibole "sponge"
928 in arc crust? Geology 35, 787-790.

929 Davidson, J., Turner, S. & Plank, T. (2013) Dy/Dy*: Variations Arising from Mantle Sources and
930 Petrogenetic Processes. Journal of Petrology 54, 525-537.

931 De Kerneizon, M.L., Bellon, H., Carron, J.P. & Maury, R.C. (1983). The island of St-Lucia-
932 petrochemistry and geochronology of the main magmatic series. Bulletin de la Société Géologique
933 de France 25, 845-853.

934 DePaolo, D.J. (1981). Trace element and isotopic effects of combined wallrock assimilation and
935 fractional cristallization. Earth and Planetary Science Letters 53, 189-202.

936 Dostal, J., Dupuy, C., Carron, J.P., Le Guen de Kerneizon, M. & Maury, R.C. (1983). Partition
937 coefficients of trace elements: application to volcanic rocks of St Vincent, West Indies.
938 Geochimica Cosmochimica Acta 47, 525-533.

939 Dufrane, S.A., Turner, S., Dosseto, A. & Van Soest, M. (2009). Reappraisal of fluid and sediment
940 contributions to Lesser Antilles magma. Chemical Geology 265, 272-278.

941 Fujimaki, H., Tatsumoto, M. & Aoki, K. (1984). Partition coefficients of Hf, Zr and REE between
942 phenocrysts and groundmasses. Proceedings of the fourteenth lunar and planetary science
943 conference, Part 2. Journal of Geophysical Research 89, B662-B672.

944 Galer, S.J.G. (1997). Optimal triple spiking for high precision lead isotope ratio determination.
945 Terra Nova, 9: p. 441.

946 Germa, A., Quidelleur, X., Labanieh, S., Chauvel, C. & Lahitte, P. (2011). The volcanic evolution
947 of Martinique Island: Insights from K-Ar dating into the Lesser Antilles arc migration since the
948 Oligocene. Journal of Volcanology and Geothermal Research 208, 122-135.

949 Green, T.H., Sie, S.H., Ryan, C.G. & Cousens, D.R. (1989). Proton microprobe-determined
950 partitioning of Nb, Ta, Zr, Sr and Y between garnet, clinopyroxene and basaltic magma at high
951 pressure and temperature. Chemical Geology 74, 201-216.

952 Heath, E., Macdonald, R., Belkin, H., Hawkesworth, C. & Sigurdsson, H. (1998). Magmagenesis
953 at Soufrière Volcano, Lesser Antilles Arc. Journal of Petrology 39, 1721-1764.

954 Hermann, J. & Rubatto, D. (2009). Accessory phase control on the trace element signature of
955 sediment melts in subduction zones. Chemical Geology 265, 512-526.

956 Huang, F., Lundstrom, C.C., Sigurdsson, H. & Zhang, Z. (2011). U-series disequilibria in Kick'em
957 Jenny submarine volcano lavas: A new view of time-scales of magmatism in convergent margins.
958 Geochimica et Cosmochimica Acta 75, 195-212.

959 Irvine, T.N. & Baragar, W.R.A. (1971). A guide to the chemical classification of the common
960 volcanic rocks. Canadian Journal of Earth Sciences 8, 523-548.

961 Johnson, M.C. & Plank, T. (1999). Dehydration and melting experiments constrain the fate of
962 subducted sediments. Geochemistry, Geophysics, Geosystems, doi: 10.1029/1999GC000014

963 Labanieh, S., Chauvel, C., Germa, A., Quidelleur, X. & Lewin, E. (2010). Isotopic hyperbolas
964 constrain sources and processes under the Lesser Antilles arc. Earth and Planetary Science Letters
965 298, 35-46.

966 Labanieh, S., Chauvel, C., Germa, A. & Quidelleur, X. (2012). Martinique: a clear case for
967 sediment melting and slab dehydration as a function of distance to the trench 53, 244-2464.

968 Lindsay, J.M., Trumbull, R.B., Schmitt, A.K., Stockli, D.F., Shane, P. & Howe, T. (2013).
969 Volcanic stratigraphy and geochemistry of the Soufrière Volcanic Center, Saint Lucia with
970 implications for volcanic hazards. Journal of Volcanology and Geothermal Research 258, 126-
971 142.

972 Macdonald, R., Hawkesworth, C.J. & Heath, E. (2000). The Lesser Antilles volcanic chain: a study
973 in arc magmatism. Earth-Science Reviews 49, 1-76.

974 McCann, W.R. & Sykes, L.R. (1984). Subduction of aseismic ridges beneath the Caribbean plate:
975 Implications for the tectonics and seismic potential of the Northeastern Caribbean. Journal of
976 Geophysical Research 89, 4493-4519.
977 McKenzie, D. & O'Nions, R.K. (1991). Partial Melt Distributions from Inversion of Rare Earth
978 Element Concentrations. Journal of Petrology 32, 1021-1091.

979 Nowell, G.M., Kempton, P.D., Noble, S.R., Fitton, J.G., Saunders, A.D., Mahoney, J.J. & Taylor,
980 R.N. (1998). High precision Hf isotope measurements of MORB and OIB by thermal ionisation
981 mass spectrometry: insights into the depleted mantle. Chemical Geology 149, 211-233.

OAS (Organization of American States) (1984). St. Lucia Geology Map. St. Lucia development Atlas. Department of Regional Development, Saint Lucia Development Atlas.

Ottley, C.J., Pearson, D.G. & Irvine, G.J. (2003). A routine method for the dissolution of geological samples for the analysis of REE and trace elements via ICP-MS. Plasma Source Mass Spectrometry. Special Publication of the Royal Society of Chemistry, pp 221-230.

Paster, T.P., Schauwecker, D.S. & Haskin, L.A. (1974). The behaviour of some trace elements during solidification of the Skaergaard layered series. Geochimica Cosmochimica Acta 38, 1549-1577.

Plank, T. & Langmuir, C.H. (1998). The chemical composition of the subducting sediment and its consequences for the crust and mantle. Chemical Geology 145, 325-394.

Rudnick, R.L. & Fountain, D.M. (1995). Nature and composition of the continental crust: a lower crustal perspective. Review in Geophysics 33, 267-309.

Salters, V.J.M. & Longhi, J. (1999). Trace element partitioning during the initial stages of melting beneath mid-ocean ridges. Earth and Planetary Science Letters 166, 15-30.

Samper, A., Quidelleur, X., Boudon, G., Le Friant, A. & Komorowski, J.C. (2008). Radiometric dating of three large volume flank collapses in the Lesser Antilles Arc. Journal of Volcanology and Geothermal Research 176, 485-492.

Schmitt, A.K., Stockli, D.F., Lindsay, J.M., Robertson, R., Lovera, O.M. & Kislitsyn, R. (2010). Episodic growth and homogenization of plutonic roots in arc volcanoes from combined U-Th and (U-Th)/He zircon dating. Earth and Planetary Science Letters 295, 91-103.

1002 Sherman, S. B. (1992). Geochemistry and petrogenesis of Saba, Lesser Antilles. MSc thesis,
1003 University of South Florida, Tampa, pp 114.

1004 Smith, D.J. (2014). Clinopyroxene precursors to amphibole sponge in arc crust. Nature
1005 communications 5, doi:10.1038/ncomms5329.

1006 Smith, T.E., Thirlwall, M.F. & Macpherson, C. (1996). Trace element and Isotope Geochemistry
1007 of the Volcanic Rocks of Bequia, Grenadine Islands, Lesser Antilles Arc: a Study of Subduction
1008 Enrichment and Intra-crustal Contamination. Journal of Petrology 37, 117-143.

1009 Speed, R.C. & Walker, J.A. (1991). Oceanic-crust of the Grenada Basin in the southern Lesser
1010 Antilles arc platform. Journal of Geophysical Research-Solid Earth Planets 96, 3835-3851.

1011 Stormer, J.C. & Nicholls, J. (1978). XLFRAC; a program for the interactive testing of magmatic
1012 differentiation models. Computer Geosciences 4, 143-159.

1013 Sun, S.S. & McDonough, W. (1989). Chemical and isotopic systematics of ocean arc basalts:
1014 implications for mantle composition and processes. In: Saunders, A. D. & Norry, M. J. (ed)
1015 Magmatism in the Ocean Basins. Geological Society of London Special Publication 42, pp 313-
1016 345.

1017 Thirlwall, M.F. & Graham, A.M. (1984). Evolution of high-Ca, high-Sr C-series basalts from
1018 Grenada, Lesser Antilles: Contamination in the arc crust. Journal of the Geological Society of
1019 London 141, 427-445.

1020 Thirlwall, M.F., Graham, A.M., Arculus, R.J., Harmon, R.S. & Macpherson, C.G. (1996).
1021 Resolution of the effects of crustal assimilation, sediment subduction, and fluid transport in island

1022 arc magmas: Pb-Sr-Nd-O isotope geochemistry of Grenada, Lesser Antilles. Geochimica
1023 Cosmochimica Acta 60, 4785-4810.

1024 Tollan, P.M.E., Bindeman, I. & Blundy, J.D. (2012). Cumulate xenoliths from St. Vincent, Lesser
1025 Antilles Island Arc: a window into upper crustal differentiation of mantle-derived basalts.
1026 Contributions to Mineralogy and Petrology 163, 189-208.

1027 Toothill, J., Williams, C.A., Macdonald, R., Turner, S.P., Rogers, N.W., Hawkesworth, C.J.,
1028 Jerram, D.A., Ottley, C.J. & Tindle, A.G. (2007). A complex petrogenesis for an arc magmatic
1029 suite, St Kitts, Lesser Antilles. Journal of Petrology 48, 3-42.

1030 Turner, S., Hawkesworth, C., Van Calsteren, P., Heath, E., Macdonald, R. & Black, S. (1996). U-
1031 series isotopes and destructive plate margin magma genesis in the Lesser Antilles. Earth and
1032 Planetary Science Letters 142, 191-207.

1033 Van Soest, M.C. (2000). Sediment Subduction and Crustal Contamination in the Lesser Antilles
1034 Island Arc. PhD thesis, University of Vrije, Amsterdam, pp 287.

1035 Van Soest, M.C., Hilton, D.R., Macpherson, C.G. & Mattey, D.P. (2002). Resolving sediment
1036 subduction and crustal contamination in the Lesser Antilles arc: a combined He–O–Sr Isotope
1037 approach. Journal of Petrology 43, 143-170.

1038 Vervoort, J.D., Patchett, P.J., Blichert-Toft, J. & Albarede, F. (1999). Relationships between Lu-
1039 Hf and Sm-Nd isotopic systems in the global sedimentary system. Earth and Planetary Science
1040 Letters 168, 79-99.

1041 Wadge, G. & Shepherd, J.B. (1984). Segmentation of the Lesser Antilles subduction zone. Earth
1042 and Planetary Science Letters 71, 297-304.

1043 Weis, D., Kieffer, B., Hanano, D., Silva, I.N., Barling, J., Pretorius, W., Maerschalk, C. & Mattielli
1044 (2007). Hf isotope composition of U.S. Geological Survey reference materials. Geochemistry,
1045 Geophysics, Geosystems 8, Q06006

1046 White, W.M. & Dupré, B. (1986). Sediment Subduction and Magma Genesis in the Lesser
1047 Antilles: Isotopic and Trace Element Constraints. Journal of Geophysical Research 91, 5927-5941.

1048 White, W.M., Dupré, B. & Vidal, P. (1985). Isotope and trace element geochemistry of sediments
1049 from the Barbados Ridge–Demerara Plain region, Atlantic ocean. Geochimica Cosmochimica
1050 Acta 49, 1875-1886.

1051 Woodhead, J.D., Hergt, J.M., Davidson, J.P. & Eggins, S.M. (2001). Hafnium: isotope evidence
1052 for 'conservative' element mobility during subduction zone processes. Earth and Planetary Science
1053 Letters 192, 331-346.

1054 Workman, R.K. & Hart, S.R. (2005). Major and trace element composition of the depleted MORB
1055 mantle (DMM). Earth and Planetary Science Letters 231, 53-72.

1056 Zack, T., & Brumm, R. (1998). Ilmenite/liquid partition coefficients of 26 trace elements
1057 determined through ilmenite/clinopyroxene partitioning in garnet pyroxenites. Seventh
1058 International Kimberlite Conference, Cape Town, pp. 986-988.

1059 **FIGURE CAPTIONS**

1060 Fig. 1: (a) Location of St Lucia on a bathymetric contour map of the Lesser Antilles arc area
1061 modified from Bezard et al. (2014). The location all the islands of the arc, of the Grenada and
1062 Tobago basins, as well as The Barbados and St Lucia ridges and the DSDP sites 543 and 144 are
1063 also shown (b) geological map of St Lucia modified from Lindsay et al. (2013).

Fig. 2: Comparison of Sr, Nd isotopic composition of St Lucia lavas to all the other lavas from the rest of the arc. St Lucia compositions cover most of the arc variations. Data sources; Saba, (Sherman, 1992; Van Soest, 2000; Dufrane et al. 2009), Statia (Davidson, 1984;Van Soest, 2002), St Kitts (Toothhill et al., 2007;Van Soest, 2000), Nevis (Van Soest, 2000); Redonda (Davidson, 1984), Montserrat (Davidson, 1984; Van Soest, 2000), Guadeloupe (Van Soest, 2000; Dominica (Davidson, 1984), Martinique (Davidson, 1984; Labanieh et al., 2010; Van Soest, 2000), St Lucia (Bezard et al., 2014), St Vincent (Heat et al., 1998; Van Soest, 2000), Grenadine with Bequia (Smith et al., 1996), Ile de Caille (Van Soest, 2000; Turner et al., 1996) and Kick'em Jenny (Huang et al., 2011), and Grenada (Thirlwall and Graham, 1984; Thirlwall et al., 1996; Van Soest, 2000). MORB field is mid-Atlantic Ridge mafic volcanic rocks between 30°N and 30°S (data from PETDB: http://petdb.org/science.jsp/). 144, 543 and correspond to Atlantic sediments cored at the front of the trench at DSDP sites 144, 543 and Barbados corresponds to sediments outcropping on Barbados; Carpentier et al., 2008, 2009).

Fig. 3: Rare earth element (a, c, e) and expanded trace element (b, d, f) composition of Pre-SVC1, Pre-SVC2 and SVC lavas normalised to chondrite C1 of Sun and McDonough (1989). Insets show the position of the Pre-SVC1, 2 and SVC Sr-Nd isotopic composition compared to MORB; sediments from sites DSDP 543 and 144 and arc field shown in Fig. 2.

Fig. 4: Sr, Nd, Hf, Pb isotopic composition of St Lucia lavas with AFC models. See text for description of parameters used. Full model parameters and data are presented in Supplementary data file 1. SL-83-25 with am = AFC model using SL-83-25 isotopic composition and least square

model #2. SL-83-25 no am = AFC model using SL-83-25 isotopic composition and least square model #1. SL-83-44 with am/no am models use the isotopic composition of SL-83-44 lava. F = amount of residual melt. MORB, local sediment fields as well as the bulk sediment of each locality) are also shown (data source as in Fig. 2). B Bar, B 543 and B 144 = the bulk sediment composition of Barbados, DSDP site 543 and DSDP site 144 respectively. Red and black striped pentagons represent the assimilant composition. The terrestrial array in panel (a) is from Vervoort et al. (1999). The inset in panel (d) shows the very radiogenic Pb composition of the black shales from DSDP site 144, making them unlikely to be the assimilant.

Fig. 5: Hf, Nd, Sr, Pb isotopes and La/Sm and Th/Th* vs. SiO_2 (wt. %) in St Lucia lavas. Pre-SVC2 and SVC composition vary exactly the same way in all the proxies with increasing SiO_2 (wt. %) while Pre-SVC1 lava compositions remain similar in isotope and trace element ratios during differentiation. Sr, Nd and Pb isotope ratios are from Bezard et al. (2014). Impact on La/Sm and Th/Th* of mineral fractionation of assemblages obtained by least square models is presented in e and f. Tick marks on the arrows represent the amount of fractionation and the black dot on each arrow represent the percentage of phases fractionated for the best fit. Impact of AFC on La/Sm and Th/Th* is presented in g where tick marks correspond to the amount of melt remaining (see text and Supplementary data file 1 for model parameters).

Fig. 6: Major element variation of St Lucia lavas. (a) AFM diagram with dividing line from Irvine and Baragar (1971) (b) MgO, (c) CaO, (d) Al_2O_3, (e) TiO_2, (f) K_2O and (g) FeO_{tot} variations are plotted against SiO_2 and. Least square models #2 and #3 are also presented (#1 is not shown here but is similar to #2).Tick marks on the arrows represent the amount of fractionation and the black

dot on each arrow represent the amount of phases fractionated for the best fit of the least square models.

Fig. 7: Mixing models to constrain the amount of sediment involved in the source of Pre-SVC1 lavas. Model 1 (Site 144 conc.) = model in which Sr, Nd, Hf and Pb concentrations of the bulk of site 144 compositions were used. Model 2 (Site 543 conc.) = model in which Sr and Nd concentrations in the bulk site 543 compositions were used. Models 1' and 2' use the same parameters as Models 1 and 2, respectively, except for the $^{87}Sr/^{86}Sr$ composition of the Pre-SVC1 lavas, which was shifted to 0.70508 which is the value of the most primitive picrite in Grenada (see text for explanation). $^{143}Nd/^{144}Nd$ and $^{176}Hf/^{177}Hf$ were fixed at 0.5122 and 0.2827 which are the least crustal composition found in most local sediments. The most mafic lava of every island of the arc as well as all the local sediment composition are also shown for comparison (same reference as in Fig. 2). DMM = trace element (Workman & Hart, 2005) and isotopic (White et al., 1985) composition of the depleted MORB mantle.

Fig. 8: (a) MgO (wt.%), (b) La/Sm and (c) Ba/Th vs. $^{87}Sr/^{86}Sr$, $^{143}Nd/^{144}Nd$, $^{206}Pb/^{204}Pb$ of St Lucia lavas compared to both the north (top 4 figures of each panel) and the South of the arc (bottom 4 figures of each panel). Grey field present in all diagrams indicates the isotopic composition of the least evolved samples in the different islands of the northern and southern arc. Same data source as in Fig. 2 for Lesser Antilles lavas.

Fig. 9: Comparison of La/Sm, Ba/Th, $^{87}Sr/^{86}Sr$, $^{143}Nd/^{144}Nd$, $^{206}Pb/^{204}Pb$ and MgO (wt. %) of the most mafic samples analysed in each island along the arc. Primitive magma isotopic compositions

1133 from Davidson and Wilson (2011) is also shown for comparison. The grey section of the diagrams
1134 represent the central-southern section of the arc. Same data source as in Fig.2. Full compositions
1135 and names of the mafic samples used are presented in Supplementary data file 1.

Fig. 1

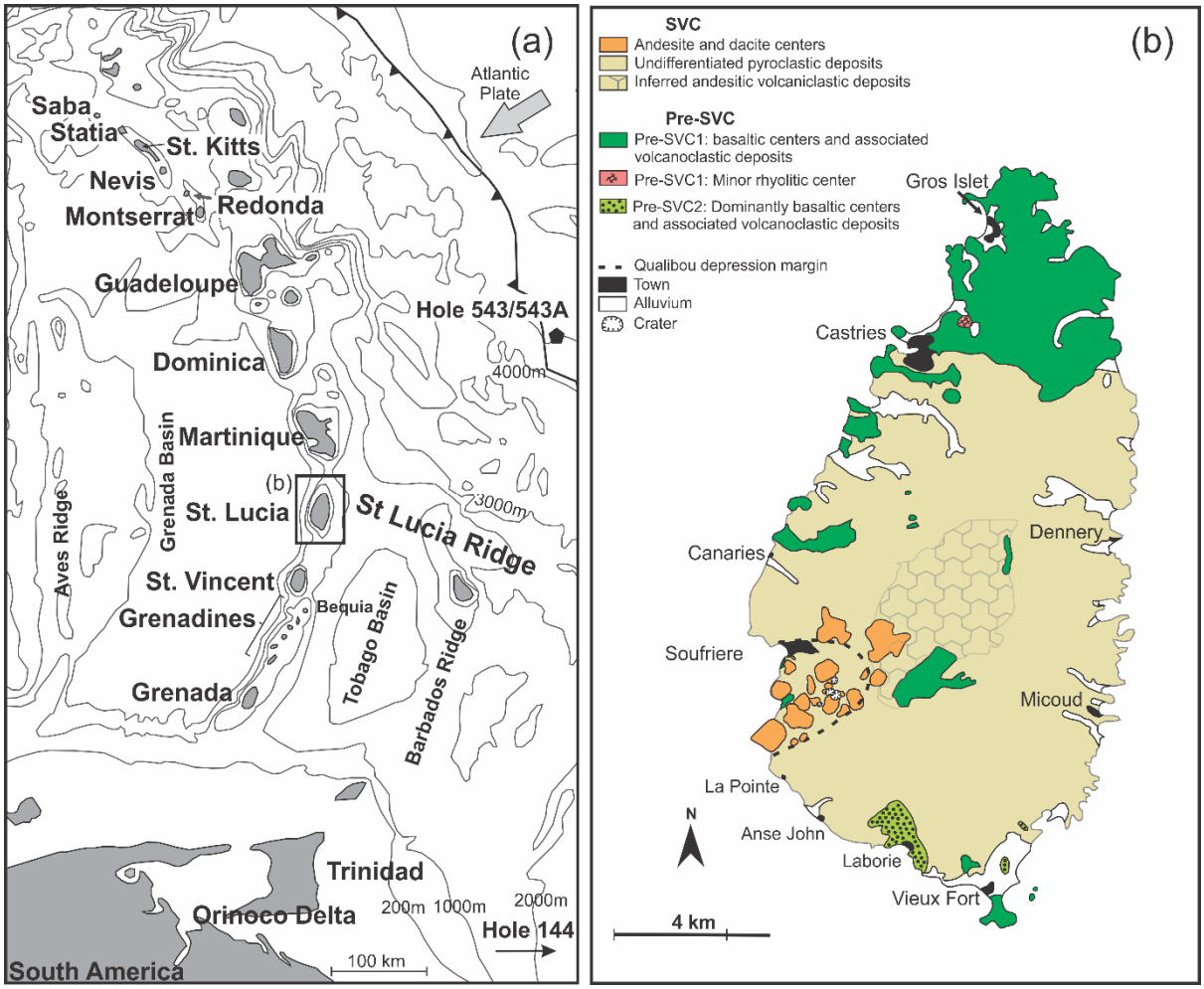
(a)
Atlantic Plate
Saba
Statia
St. Kitts
Nevis
Redonda
Montserrat
Guadeloupe
Hole 543/543A
Dominica
4000m
Martinique
Grenada Basin
Aves Ridge
(b)
St. Lucia
St Lucia Ridge
3000m
St. Vincent
Grenadines
Bequia
Tobago Basin
Barbados Ridge
Grenada
Trinidad
Orinoco Delta
200m 1000m 2000m
Hole 144
South America
100 km
(b)
SVC
Andesite and dacite centers
Undifferentiated pyroclastic deposits
Inferred andesitic volcaniclastic deposits
Pre-SVC
Pre-SVC1: basaltic centers and associated volcanoclastic deposits
Pre-SVC1: Minor rhyolitic center
Pre-SVC2: Dominantly basaltic centers and associated volcanoclastic deposits
Qualibou depression margin
Town
Alluvium
Crater
Gros Islet
Castries
Canaries
Dennery
Soufriere
Micoud
La Pointe
N
Anse John
Laborie
Vieux Fort
4 km

Fig. 2

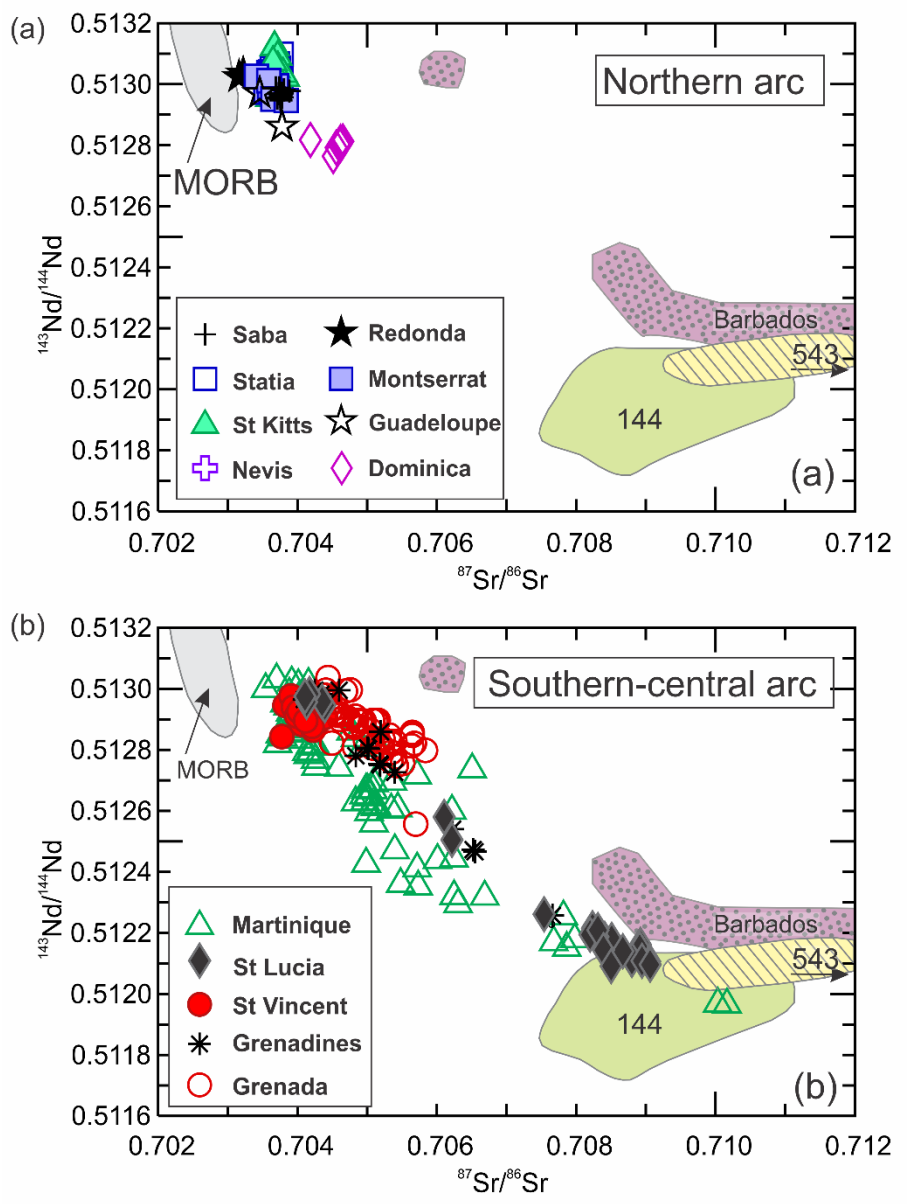
(a)
Northern arc
MORB
Saba
Redonda
Statia
Montserrat
St Kitts
Guadeloupe
Nevis
Dominica
Barbados
543
144
(a)
(b)
Southern-central arc
MORB
Martinique
St Lucia
St Vincent
Grenadines
Grenada
Barbados
543
144
(b)
$^{143}Nd/^{144}Nd$
$^{87}Sr/^{86}Sr$
0.5132
0.5130
0.5128
0.5126
0.5124
0.5122
0.5120
0.5118
0.5116
0.702
0.704
0.706
0.708
0.710
0.712

Fig. 3

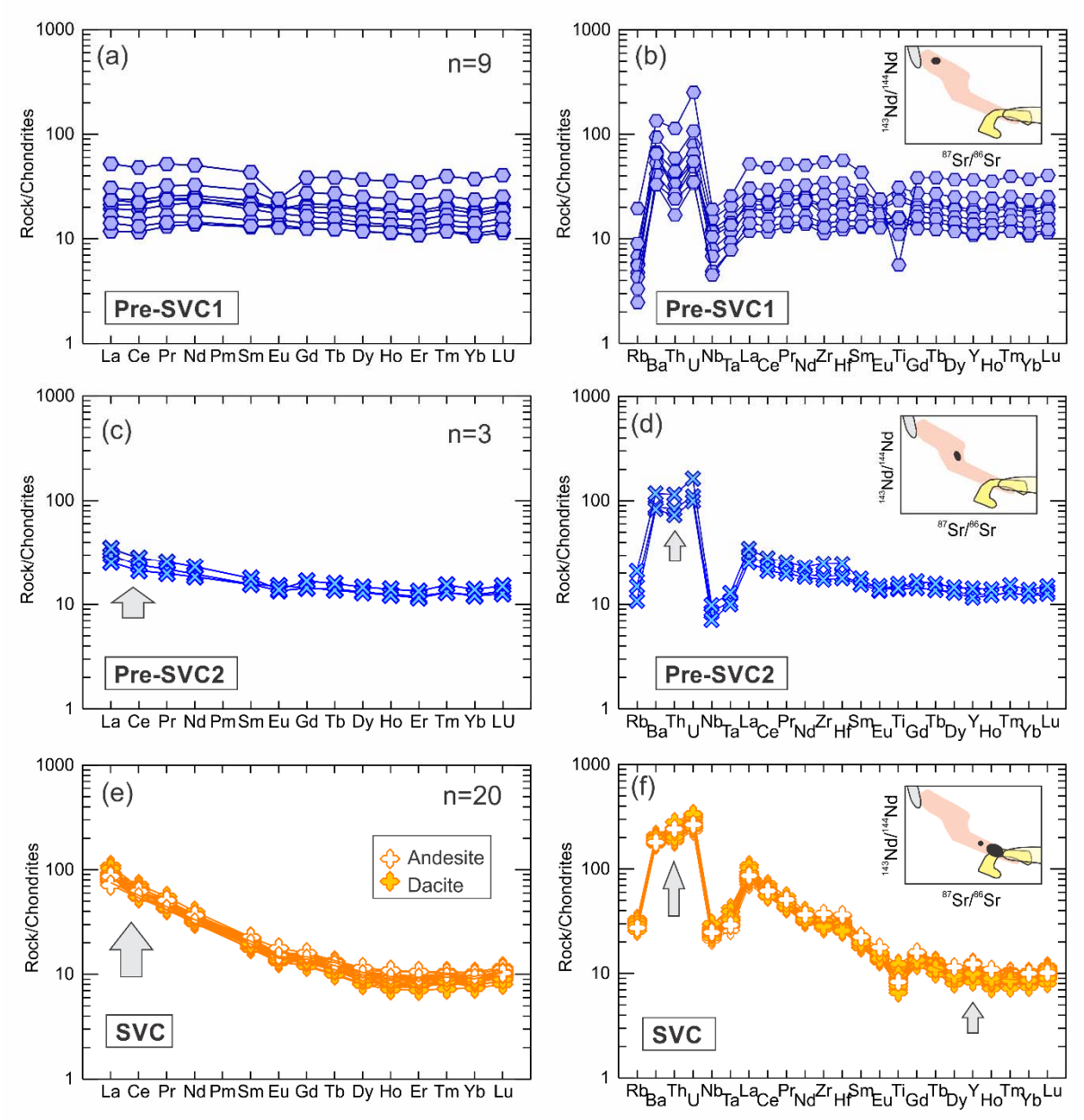
(a)
n=9
Pre-SVC1
(b)
Pre-SVC1
(c)
n=3
Pre-SVC2
(d)
Pre-SVC2
(e)
n=20
Andesite
Dacite
SVC
(f)
SVC
Rock/Chondrites
1000
100
10
1
La Ce Pr Nd Pm Sm Eu Gd Tb Dy Ho Er Tm Yb LU
Rb Ba Th U Nb Ta La Ce Pr Nd Zr Hf Sm Eu Ti Gd Tb Dy Y Ho Tm Yb Lu
143Nd/144Nd
87Sr/86Sr

Fig. 4

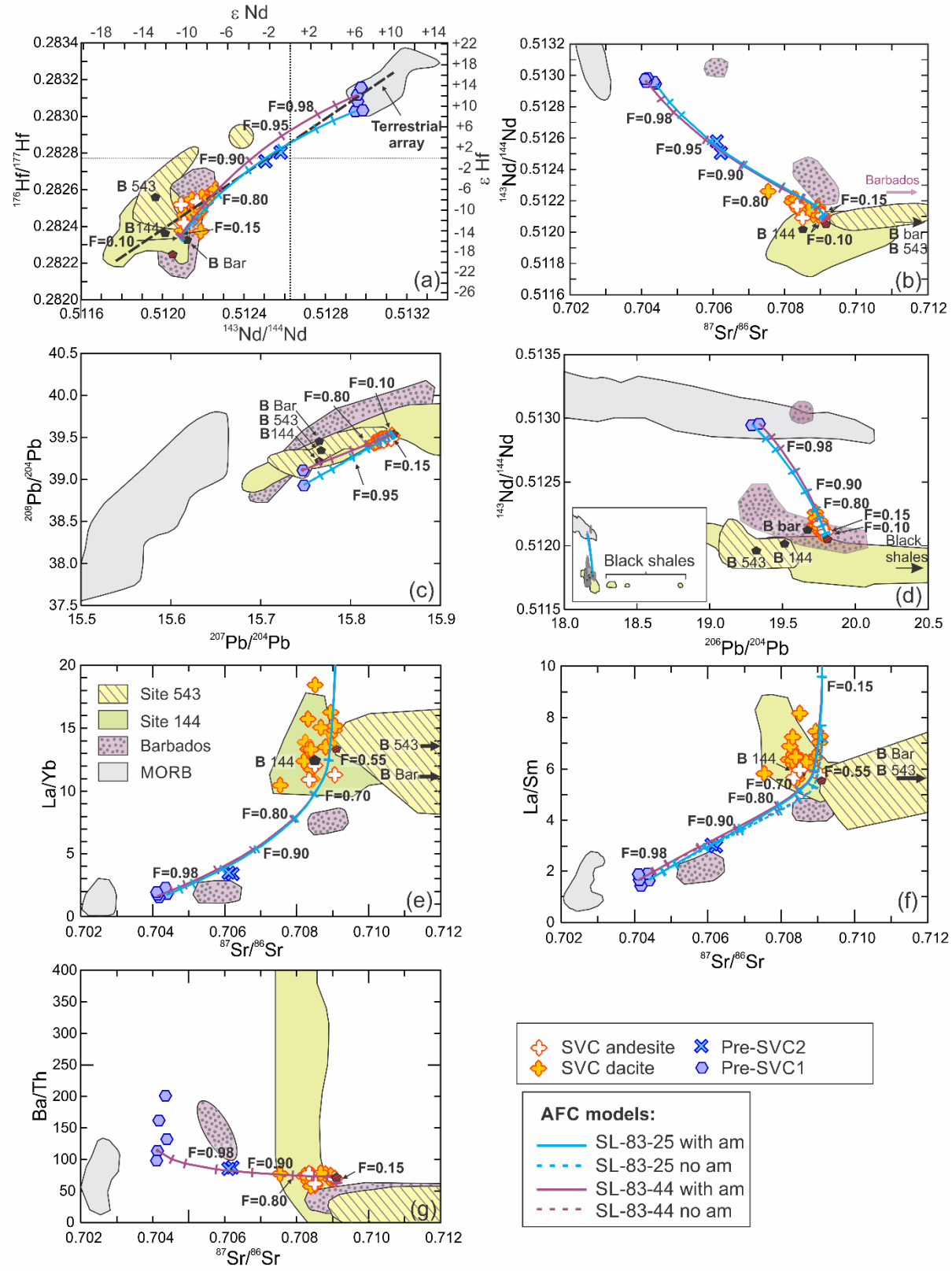
ε Nd
ε Hf
$^{176}Hf/^{177}Hf$
$^{143}Nd/^{144}Nd$
F=0.98
F=0.95
F=0.90
F=0.80
F=0.15
F=0.10
Terrestrial array
B 543
B144
B Bar
(a)
$^{143}Nd/^{144}Nd$
$^{87}Sr/^{86}Sr$
Barbados
B 144
B bar
B 543
(b)
$^{208}Pb/^{204}Pb$
$^{207}Pb/^{204}Pb$
B Bar
B 543
B144
(c)
$^{143}Nd/^{144}Nd$
$^{206}Pb/^{204}Pb$
Black shales
B bar
B 543
B 144
(d)
La/Yb
$^{87}Sr/^{86}Sr$
Site 543
Site 144
Barbados
MORB
B 144
B 543
B Bar
F=0.55
F=0.70
(e)
La/Sm
$^{87}Sr/^{86}Sr$
B 144
B Bar
B 543
F=0.55
F=0.70
F=0.80
F=0.90
F=0.98
(f)
Ba/Th
$^{87}Sr/^{86}Sr$
F=0.98
F=0.90
F=0.80
F=0.15
(g)
SVC andesite
SVC dacite
Pre-SVC2
Pre-SVC1
AFC models:
SL-83-25 with am
SL-83-25 no am
SL-83-44 with am
SL-83-44 no am

Fig. 5

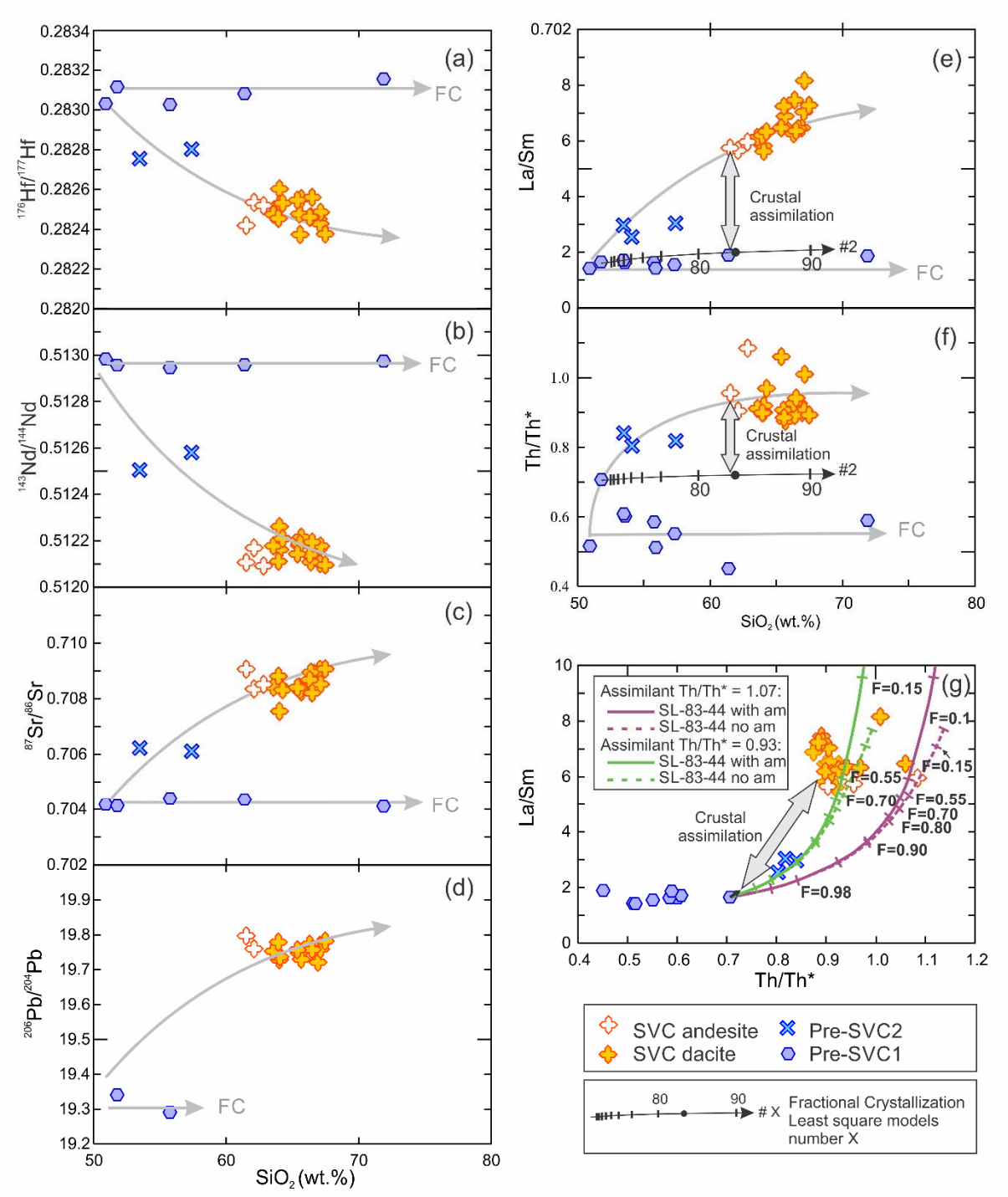
(a)
(b)
(c)
(d)
(e)
(f)
(g)
FC
Crustal assimilation
#2
80
90
$^{176}Hf/^{177}Hf$
$^{143}Nd/^{144}Nd$
$^{87}Sr/^{86}Sr$
$^{206}Pb/^{204}Pb$
La/Sm
Th/Th*
SiO_2(wt.%)
Assimilant Th/Th* = 1.07:
SL-83-44 with am
SL-83-44 no am
Assimilant Th/Th* = 0.93:
SL-83-44 with am
SL-83-44 no am
F=0.15
F=0.1
F=0.55
F=0.70
F=0.80
F=0.90
F=0.98
SVC andesite
SVC dacite
Pre-SVC2
Pre-SVC1
Fractional Crystallization
Least square models
number X

Fig. 6

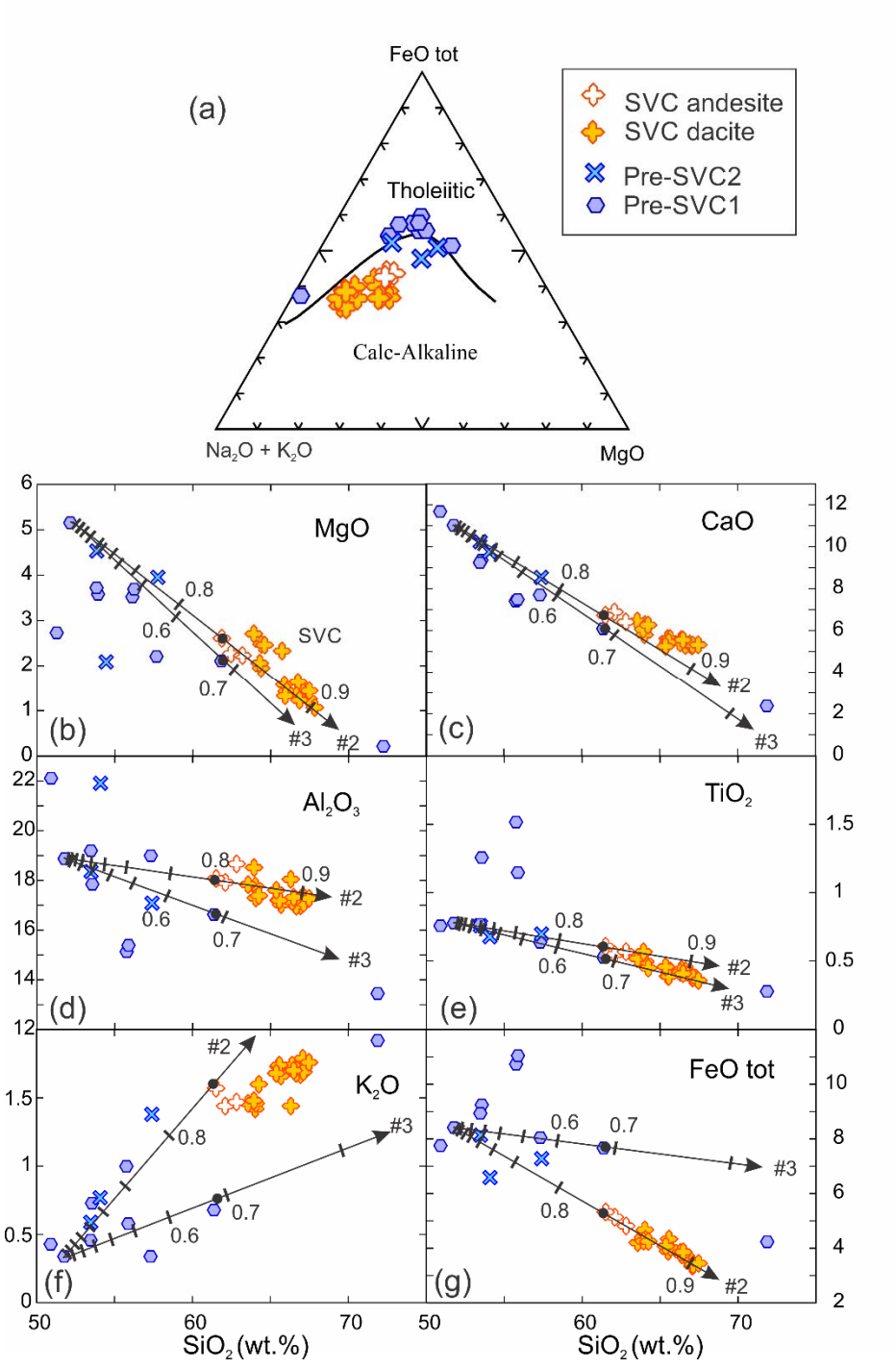
(a)
FeO tot
Tholeiitic
Calc-Alkaline
Na2O + K2O
MgO
SVC andesite
SVC dacite
Pre-SVC2
Pre-SVC1
(b)
MgO
SVC
0.6
0.7
0.8
0.9
#2
#3
(c)
CaO
(d)
Al2O3
(e)
TiO2
(f)
K2O
(g)
FeO tot
SiO2 (wt.%)
SiO2 (wt.%)

Fig. 7

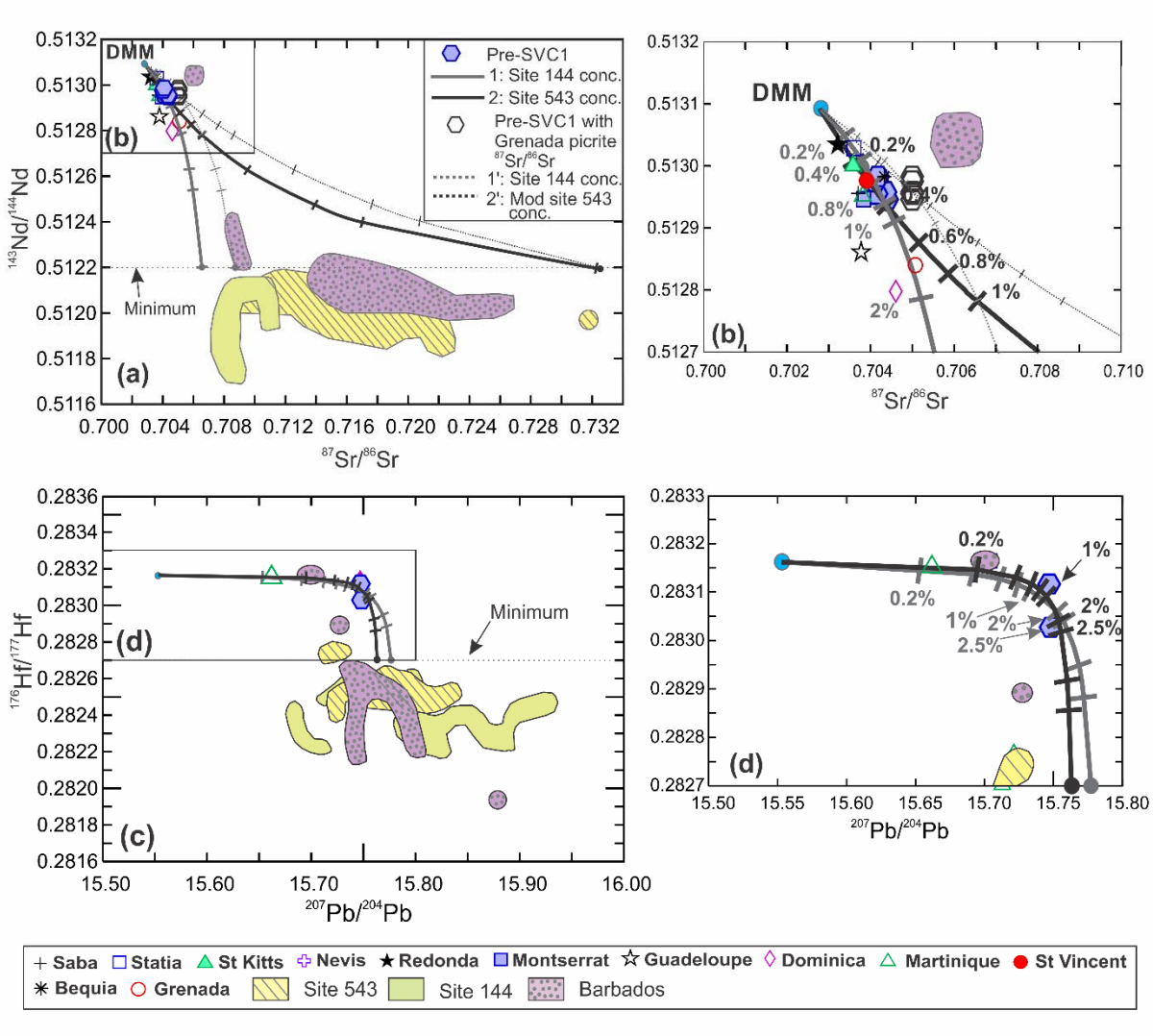
DMM
(b)
Pre-SVC1
1: Site 144 conc.
2: Site 543 conc.
Pre-SVC1 with Grenada picrite $^{87}Sr/^{86}Sr$
1': Site 144 conc.
2': Mod site 543 conc.
Minimum
(a)
$^{143}Nd/^{144}Nd$
$^{87}Sr/^{86}Sr$
0.2%
0.4%
0.8%
1%
2%
0.6%
(c)
(d)
$^{176}Hf/^{177}Hf$
$^{207}Pb/^{204}Pb$
2.5%
+ Saba
Statia
St Kitts
Nevis
Redonda
Montserrat
Guadeloupe
Dominica
Martinique
St Vincent
Bequia
Grenada
Site 543
Site 144
Barbados

Fig. 8

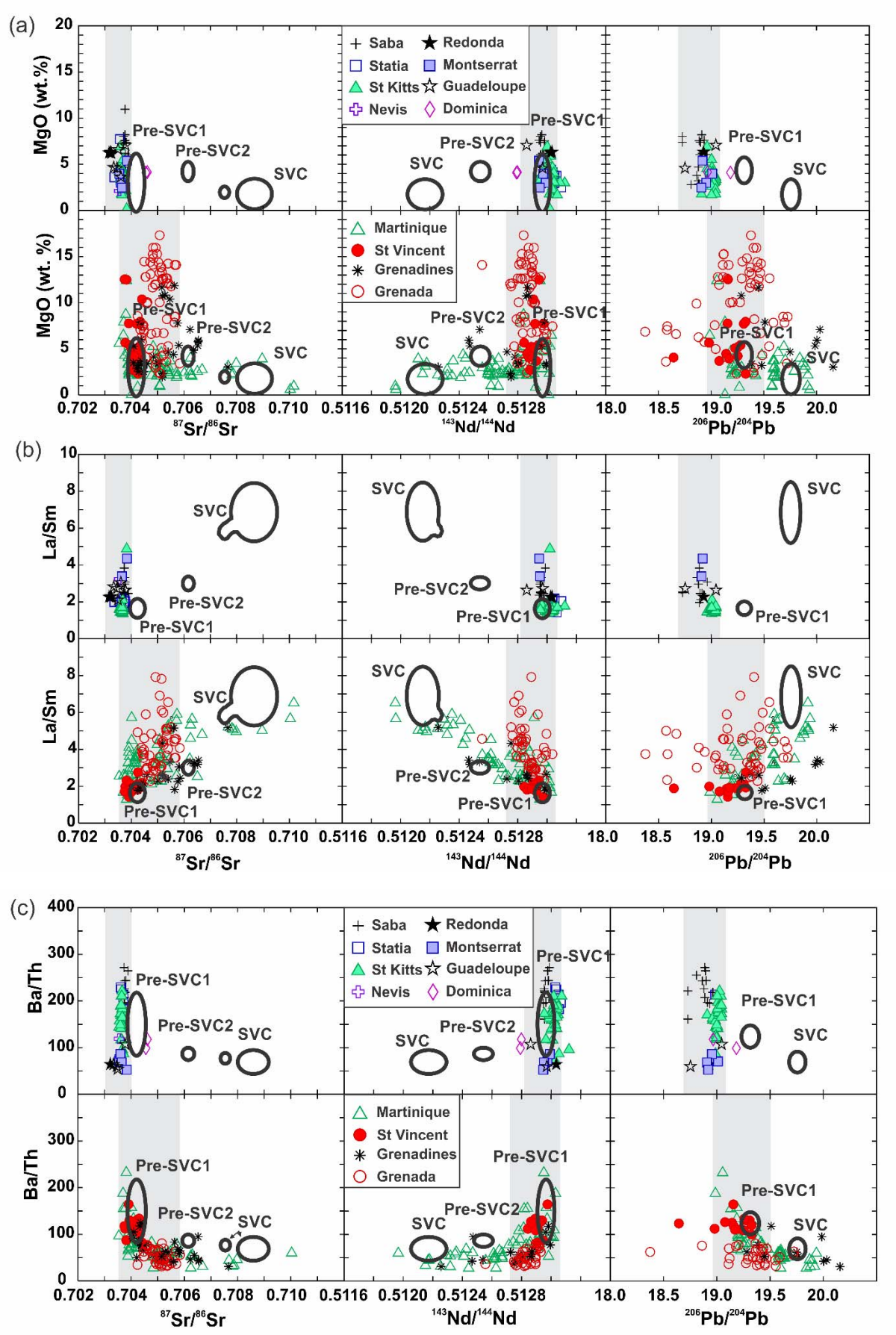
(a)
MgO (wt.%)
MgO (wt. %)
Saba
Redonda
Statia
Montserrat
St Kitts
Guadeloupe
Nevis
Dominica
Martinique
St Vincent
Grenadines
Grenada
Pre-SVC1
Pre-SVC2
SVC
$^{87}Sr/^{86}Sr$
$^{143}Nd/^{144}Nd$
$^{206}Pb/^{204}Pb$
(b)
La/Sm
(c)
Ba/Th

Fig. 9

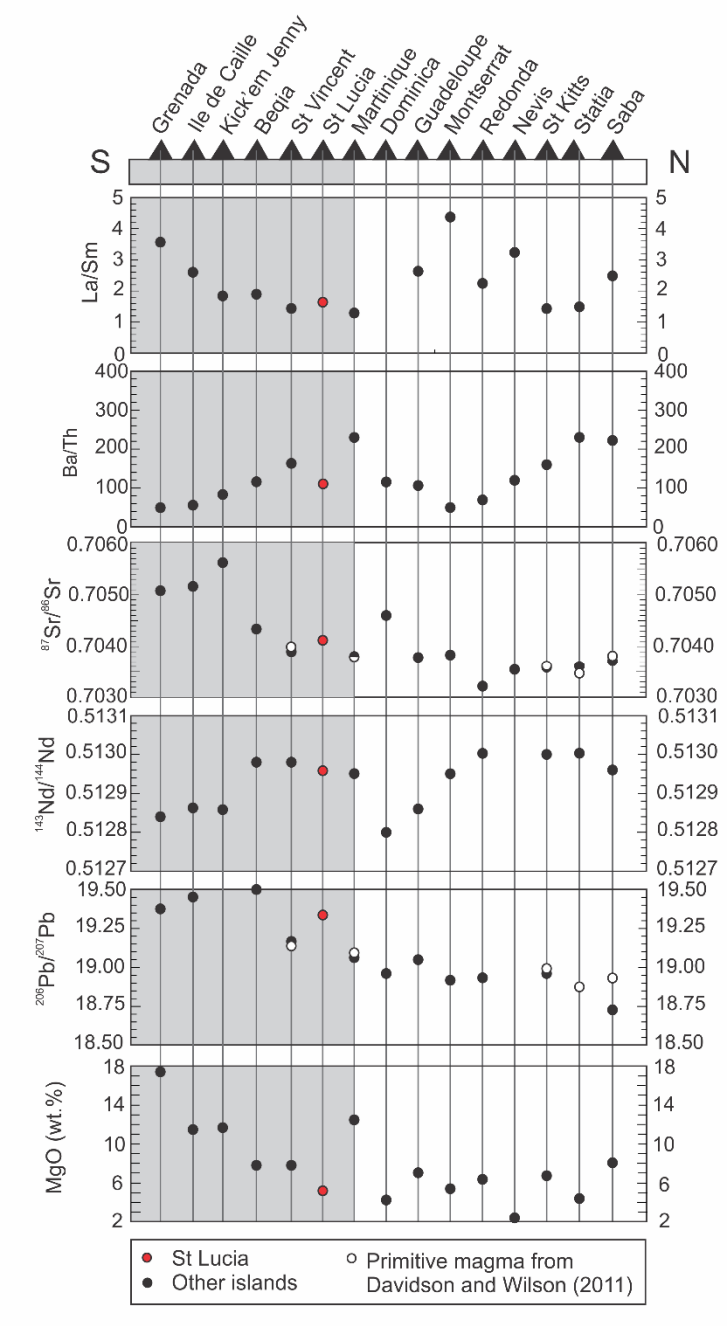
Grenada
Ile de Caille
Kick'em Jenny
Beqia
St Vincent
St Lucia
Martinique
Dominica
Guadeloupe
Montserrat
Redonda
Nevis
St Kitts
Statia
Saba
S
N
La/Sm
Ba/Th
87Sr/86Sr
143Nd/144Nd
206Pb/207Pb
MgO (wt.%)
St Lucia
Other islands
Primitive magma from
Davidson and Wilson (2011)

Table 1. Major and trace element concentrations and Sr-Nd-Pb-Hf isotopic compositions of St Lucia volcanic rocks.

Group:	**SVC**	**SVC**	**SVC**	**SVC**	**SVC**	**SVC**
Sample:	**SL8303[a]**	**SL8308[a]**	**SL8312[a]**	**SL8315[a]**	**SL8316[a]**	**SL8317[a]**
SiO_2	64.02	66.93	66.65	62.10	64.05	61.51
TiO_2	0.49	0.42	0.43	0.55	0.50	0.61
Al_2O_3	17.77	16.97	16.96	17.91	17.29	18.07
FeO tot	4.67	3.54	3.72	5.13	4.32	5.32
MnO	0.13	0.12	0.12	0.17	0.13	0.14
MgO	1.94	1.43	1.44	2.26	2.47	2.60
CaO	5.79	5.36	5.29	6.89	6.28	6.73
Na_2O	3.13	3.07	3.18	2.85	2.92	2.71
K_2O	1.42	1.67	1.68	1.44	1.46	1.57
P_2O_5	0.11	0.10	0.11	0.12	0.10	0.14
LOI	1.75	1.19	1.23	3.45	0.16	1.66
Ti	4600	4110	4031	4952	4745	5573
V	65	20.6	19.4	31.8	48.4	35.7
Ga	17.7	17.7	17.7	17.4	16.8	17.8
Rb	67.0	78.0	77.7	60.3	59.5	70.7
Sr	325	313	314	298	296	310
Y	20.1	16.3	16.2	16.4	17.6	17.7
Zr	110	128	129	117	111	128
Nb	5.4	7.4	7.2	5.2	6.3	6.8
Ba	440	515	514	411	425	425
La	18.7	21.8	22.4	16.9	17.9	19.3
Ce	33.9	41.6	44.2	33.1	34.9	37.3
Pr	4.35	4.85	5.27	3.96	4.22	4.55
Nd	16.4	17.5	18.7	14.5	15.6	16.6
Sm	3.21	3.37	3.48	3.00	3.19	3.36
Eu	0.91	0.88	0.88	0.86	0.85	0.90
Gd	3.19	3.07	3.09	2.88	3.02	3.16
Tb	0.50	0.47	0.47	0.46	0.49	0.48
Dy	2.82	2.51	2.54	2.52	2.66	2.72
Ho	0.60	0.51	0.51	0.52	0.54	0.57
Er	1.76	1.46	1.46	1.52	1.57	1.60
Tm	0.27	0.24	0.23	0.24	0.25	0.26
Yb	1.78	1.57	1.51	1.55	1.63	1.71
Lu	0.30	0.26	0.27	0.26	0.27	0.29
Hf	2.89	3.32	3.42	2.98	2.87	3.14
Ta	0.39	0.55	0.60	0.36	0.48	0.47
Pb	12.1	15.9	15.3	10.8	12.3	16.5
Th	5.7	7.2	7.3	5.3	5.7	6.1
U	2.04	2.70	2.63	1.86	1.99	2.12
La/Sm	5.81	6.46	6.44	5.66	5.62	5.74
Th/Th*	0.90	0.90	0.93	0.90	0.92	0.96
$^{143}Nd/^{144}Nd$	0.512261	0.512161	0.512147	0.512169	0.512161	0.512106
1SE	0.000005	0.000005	0.000006	0.000005	0.000005	0.000005
$^{87}Sr/^{86}Sr$	0.707542	0.708925	0.708914	0.708346	0.70843	0.709056
1SE	0.000005	0.000005	0.000005	0.000005	0.00005	0.000005
$^{206}Pb/^{204}Pb$	19.7280	19.7211	_	19.7604	19.7365	19.7967
1SE	0.0004	0.0004	_	0.0005	0.0004	0.0005
$^{207}Pb/^{204}Pb$	15.8260	15.8302	_	15.8374	15.8327	15.8449
1SE	0.0005	0.0004	_	0.0004	0.0004	0.0004
$^{208}Pb/^{204}Pb$	39.438	39.457	_	39.467	39.466	39.489
1SE	0.002	0.002	_	0.001	0.002	0.001
$^{176}Hf/^{177}Hf$	0.282603	0.282452	_	0.282535	0.282527	0.282419
1 SE	0.000003	0.000003	_	0.000003	0.000003	0.000005

Major element concentrations are from Davidson (1987) and Lindsay et al. (2013) and normalised to 100% volatile free. Sr, Nd and Pb isotope ratios are from Bezard et al. (2014). 1 SE = 1 standard error.

[a] Trace element concentrations and $^{176}Hf/^{177}Hf$ (if available) analysed at Durham University.

[b] Trace element concentrations analysed at Macquarie University and $^{176}Hf/^{177}Hf$ analysed at Durham University.

[c] Trace element concentrations and $^{176}Hf/^{177}Hf$ analysed at Macquarie University.

[d] Trace element concentrations analysed at Durham and $^{176}Hf/^{177}Hf$ analysed at Macquarie University.

*Also analysed by LA-ICPMS by Lindsay et al. (2013).

Table 1. continued

Group:	SVC	SVC	SVC	SVC	SVC	SVC
Sample:	SL8319[a]	SL8324[a]	SL-JL-22[a]	SL-JL-23[a]	SL-JL-24[a]	SL-JL-33[a]
SiO_2	65.52	65.67	63.56	63.94	67.08	67.12
TiO_2	0.39	0.43	0.52	0.57	0.38	0.38
Al_2O_3	17.20	17.02	17.83	18.51	17.36	17.07
FeO tot	3.88	4.02	4.20	4.26	3.34	3.39
MnO	0.12	0.12	0.10	0.09	0.09	0.09
MgO	1.57	1.42	2.70	2.05	1.25	1.43
CaO	5.62	5.61	6.45	6.06	5.27	5.31
Na_2O	3.44	3.48	3.06	2.89	3.31	3.40
K_2O	1.73	1.66	1.46	1.48	1.79	1.69
P_2O_5	0.10	0.11	0.13	0.15	0.13	0.12
LOI	0.37	0.90	0.40	1.28	1.51	1.58
Ti	3665	3920	5227	5482	3576	3646
V	23.2	23.2	44.0	25.8	8.4	12.2
Ga	17.1	16.2	16.7	17.8	16.3	16.6
Rb	75.3	67.0	59.3	63.7	73.4	73.8
Sr	319	287	298	309	303	292
Y	16.4	13.6	16.9	16.7	15.0	14.8
Zr	113	108	115	126	118	117
Nb	5.80	5.56	6.44	6.67	6.66	5.92
Ba	470	436	431	424	448	421
La	19.4	18.6	18.8	20.9	21.5	26.0
Ce	37.3	34.1	34.2	37.4	39.4	41.6
Pr	4.34	3.97	4.12	4.66	4.56	4.90
Nd	15.7	14.4	15.2	17.2	16.6	17.3
Sm	2.97	2.70	3.07	3.38	3.05	3.18
Eu	0.83	0.76	0.84	0.93	0.82	0.80
Gd	2.83	2.52	2.91	3.26	2.78	2.76
Tb	0.42	0.38	0.45	0.48	0.42	0.40
Dy	2.39	2.09	2.56	2.63	2.28	2.21
Ho	0.50	0.43	0.54	0.54	0.47	0.44
Er	1.45	1.25	1.54	1.53	1.34	1.30
Tm	0.24	0.21	0.25	0.24	0.22	0.21
Yb	1.59	1.34	1.60	1.55	1.45	1.41
Lu	0.28	0.22	0.28	0.25	0.25	0.24
Hf	2.94	2.83	2.94	3.23	3.07	2.99
Ta	0.48	0.45	0.46	0.45	0.49	0.45
Pb	15.4	12.5	12.2	11.6	14.5	14.4
Th	6.5	5.8	5.7	5.5	6.5	7.1
U	2.37	2.23	2.02	1.96	2.47	2.51
La/Sm	6.53	6.88	6.12	6.19	7.03	8.16
Th/Th*	0.91	0.87	0.91	0.90	0.91	1.01
$^{143}Nd/^{144}Nd$	0.512180	0.512215	0.512178	0.512111	0.512101	0.512177
1SE	0.000004	0.000015	0.000005	0.000005	0.000004	0.000004
$^{87}Sr/^{86}Sr$	0.708412	0.708237	0.708402	0.708801	0.709049	0.708511
1SE	0.000005	0.000004	0.000004	0.000004	0.000005	0.000004
$^{206}Pb/^{204}Pb$	19.7478	19.7300	19.7532	19.7791	19.7700	19.7588
1SE	0.0004	0.0004	0.0003	0.0005	0.0003	0.0004
$^{207}Pb/^{204}Pb$	15.8366	15.8280	15.8317	15.8361	15.8340	15.8324
1SE	0.0004	0.0004	0.0003	0.0005	0.0003	0.0004
$^{208}Pb/^{204}Pb$	39.479	39.446	39.471	39.479	39.484	39.473
1SE	0.002	0.001	0.001	0.002	0.001	0.002
$^{176}Hf/^{177}Hf$	0.282476	0.282554	0.282475	0.282455	0.282427	0.282485
1SE	0.000008	0.000007	0.000009	0.000005	0.000004	0.000004

Major element concentrations are from Davidson (1987) and Lindsay et al. (2013) and normalised to 100% volatile free. Sr, Nd and Pb isotope ratios are from Bezard et al. (2014). 1 SE = 1 standard error.

[a] Trace element concentrations and $^{176}Hf/^{177}Hf$ (if available) analysed at Durham University.

[b] Trace element concentrations analysed at Macquarie University and $^{176}Hf/^{177}Hf$ analysed at Durham University.

[c] Trace element concentrations and $^{176}Hf/^{177}Hf$ analysed at Macquarie University.

[d] Trace element concentrations analysed at Durham and $^{176}Hf/^{177}Hf$ analysed at Macquarie University.

*Also analysed by LA-ICPMS by Lindsay et al. (2013).

Table 1. Continued

Group:	SVC	SVC	SVC	SVC	SVC	SVC
Sample:	SL-JL-51[a]	SL-JL-57[a]	SL-JL-61[a*]	SL-JL-79[a*]	SL-JL-83[a]	SL-JL-84[a]
SiO_2	66.39	66.30	67.47	65.57	66.49	64.25
TiO_2	0.44	0.42	0.36	0.39	0.41	0.45
Al_2O_3	17.14	18.04	17.27	17.20	17.31	17.38
FeO tot	3.75	3.84	3.44	4.33	3.86	4.24
MnO	0.10	0.09	0.08	0.11	0.10	0.10
MgO	1.63	1.32	1.06	1.32	1.22	2.45
CaO	5.57	5.42	5.32	5.45	5.55	6.26
Na_2O	3.12	3.04	3.13	3.77	3.24	3.15
K_2O	1.74	1.44	1.76	1.74	1.70	1.60
P_2O_5	0.12	0.08	0.11	0.12	0.11	0.11
LOI	0.71	1.99	1.29	1.60	0.14	0.46
Ti	4120	3125	3325	3389	4366	3782
V	21.6	10.9	7.0	10.9	42.5	19.9
Ga	16.8	17.1	16.6	16.2	16.6	17.2
Rb	77.4	69.5	73.6	71.7	70.7	73.5
Sr	295	299	309.20	296	298	315
Y	16.5	15.2	14.9	13.1	15.3	16.1
Zr	125	113	115	115	104	110
Nb	7.43	6.13	6.34	5.62	5.44	5.82
Ba	510	489	454	454	430	476
La	24.5	20.0	21.5	19.8	18.3	19.2
Ce	39.3	38.2	37.8	34.8	33.8	39.0
Pr	4.62	4.65	4.53	4.08	4.11	4.51
Nd	16.9	16.9	16.2	14.6	14.9	16.4
Sm	3.28	3.19	2.96	2.74	2.88	3.03
Eu	0.80	0.85	0.83	0.78	0.78	0.80
Gd	3.01	2.91	2.69	2.46	2.71	2.82
Tb	0.44	0.43	0.40	0.37	0.41	0.42
Dy	2.44	2.28	2.23	2.03	2.27	2.29
Ho	0.50	0.46	0.46	0.41	0.46	0.48
Er	1.42	1.30	1.32	1.17	1.33	1.37
Tm	0.23	0.21	0.22	0.19	0.22	0.22
Yb	1.50	1.33	1.42	1.26	1.47	1.44
Lu	0.25	0.22	0.24	0.20	0.24	0.25
Hf	3.17	2.91	2.96	2.87	2.66	2.75
Ta	0.55	0.43	0.48	0.42	0.41	0.41
Pb	14.4	13.1	14.3	13.2	11.6	13.5
Th	6.8	6.2	6.4	6.0	5.9	6.6
U	2.53	2.09	2.47	2.24	2.01	2.20
La/Sm	7.46	6.26	7.27	7.24	6.35	6.33
Th/Th*	0.89	0.93	0.89	0.88	0.94	0.97
$^{143}Nd/^{144}Nd$	0.512108	0.512140	0.512096	0.512187	0.512194	0.512209
1SE	0.000003	0.000005	0.000005	0.000004	0.000005	0.000005
$^{87}Sr/^{86}Sr$	0.708946	0.708672	0.709063	0.708313	0.708202	0.708313
1SE	0.000004	0.000006	0.000004	0.000005	0.000004	0.000005
$^{206}Pb/^{204}Pb$	19.7661	19.7729	19.782	_	19.7576	_
1SE	0.0003	0.0005	0.001	_	0.0004	_
$^{207}Pb/^{204}Pb$	15.8342	15.8399	15.846	_	15.8354	_
1SE	0.0003	0.0004	0.0009	_	0.0004	_
$^{208}Pb/^{204}Pb$	39.484	39.489	39.528	_	39.483	_
1SE	0.002	0.001	0.003	_	0.002	_
$^{176}Hf/^{177}Hf$	0.282462	0.282460	0.282376	0.282373	0.282560	0.282530
1SE	0.000004	0.000004	0.000006	0.000006	0.000006	0.000004

Major element concentrations are from Davidson (1987) and Lindsay et al. (2013) and normalised to 100% volatile free. Sr, Nd and Pb isotope ratios are from Bezard et al. (2014). 1 SE = 1 standard error.

[a] Trace element concentrations and $^{176}Hf/^{177}Hf$ (if available) analysed at Durham University.

[b] Trace element concentrations analysed at Macquarie University and $^{176}Hf/^{177}Hf$ analysed at Durham University.

[c] Trace element concentrations and $^{176}Hf/^{177}Hf$ analysed at Macquarie University.

[d] Trace element concentrations analysed at Durham and $^{176}Hf/^{177}Hf$ analysed at Macquarie University.

*Also analysed by LA-ICPMS by Lindsay et al. (2013).

Table 1. Continued

Group:	SVC	SVC	Pre-SVC2	Pre-SVC2	Pre-SVC2	Pre-SVC1
Sample:	SL-JL-1[b]	SL-JL-2[c]	SL8326[d]	SL8338[a]	SL8339[d]	SL8323[a]
SiO_2	65.37	62.82	53.47	54.08	57.39	53.55
TiO_2	0.46	0.57	0.76	0.68	0.70	1.26
Al_2O_3	17.60	18.66	18.35	21.91	17.08	17.84
FeO tot	4.07	4.81	8.13	6.58	7.27	9.24
MnO	0.10	0.11	0.20	0.16	0.18	0.17
MgO	2.32	2.22	4.52	2.08	3.94	3.57
CaO	5.25	6.41	10.24	9.76	8.53	9.36
Na_2O	3.01	2.80	2.76	3.16	2.64	3.10
K_2O	1.68	1.47	0.59	0.77	1.38	0.73
P_2O_5	0.12	0.14	0.08	0.08	0.07	0.16
LOI	1.48	1.25	0.33	1.00	1.24	1.59
Ti	2922	3706	6999	6186	6388	11690
V	44.6	44.5	235	132	198	292
Ga	17.8	18.7	15.6	16.9	15.4	17.2
Rb	68.5	63.5	34.6	25.1	48.6	13.5
Sr	251	288	195	238	174	193
Y	15.7	19.5	19.7	18.2	22.3	30.3
Zr	140	145	71.7	66.6	96	105
Nb	6.02	6.12	2.06	1.74	2.42	3.00
Ba	472	436	211	199	283	163
La	19.6	20.5	7.05	6.00	8.22	5.74
Ce	38.6	38.0	14.6	12.8	17.1	14.4
Pr	4.49	4.86	2.06	1.87	2.43	2.44
Nd	15.6	17.2	9.1	8.6	10.7	12.1
Sm	3.03	3.44	2.38	2.36	2.71	3.55
Eu	0.92	1.04	0.78	0.87	0.80	1.12
Gd	2.78	3.30	2.92	2.95	3.43	4.44
Tb	_	_	0.52	0.51	0.59	0.79
Dy	2.44	2.93	3.34	3.27	3.70	5.08
Ho	0.51	0.62	0.70	0.69	0.79	1.09
Er	1.46	1.76	1.98	1.90	2.20	3.06
Tm			0.33	0.33	0.39	0.53
Yb	1.47	1.70	2.08	2.04	2.35	3.21
Lu	0.23	0.26	0.34	0.32	0.38	0.53
Hf	3.78	3.90	2.03	1.89	2.63	2.86
Ta	0.46	0.41	0.15	0.14	0.18	0.23
Pb	15.4	12.2	4.89	3.60	6.55	4.13
Th	8.2	7.0	2.41	2.11	3.32	1.28
U	2.70	2.14	0.88	0.79	1.30	0.63
La/Sm	6.47	5.95	2.97	2.54	3.04	1.62
Th/Th*	1.06	1.08	0.84	0.80	0.82	0.60
$^{143}Nd/^{144}Nd$	0.512143	0.512091	0.512505	_	0.512580	_
1 SE	0.000002	0.000003	0.000007	_	0.000006	_
$^{87}Sr/^{86}Sr$	0.708393	0.708504	0.706219	_	0.706106	_
1 SE	0.000002	0.000002	0.000003	_	0.000002	_
$^{206}Pb/^{204}Pb$	19.7568	_	_	_	_	_
1 SE	0.0007	_	_	_	_	_
$^{207}Pb/^{204}Pb$	15.8376	_	_	_	_	_
1 SE	0.0007	_	_	_	_	_
$^{208}Pb/^{204}Pb$	39.489	_	_	_	_	_
1 SE	0.002	_	_	_	_	_
$^{176}Hf/^{177}Hf$	0.282546	0.282519	0.282755	_	0.282802	_
1 SE	0.000003	0.000005	0.000005	_	0.000007	_

Major element concentrations are from Davidson (1987) and Lindsay et al. (2013) and normalised to 100% volatile free. Sr, Nd and Pb isotope ratios are from Bezard et al. (2014). 1 SE = 1 standard error.

[a] Trace element concentrations and $^{176}Hf/^{177}Hf$ (if available) analysed at Durham University.

[b] Trace element concentrations analysed at Macquarie University and $^{176}Hf/^{177}Hf$ analysed at Durham University.

[c] Trace element concentrations and $^{176}Hf/^{177}Hf$ analysed at Macquarie University.

[d] Trace element concentrations analysed at Durham and $^{176}Hf/^{177}Hf$ analysed at Macquarie University.

*Also analysed by LA-ICPMS by Lindsay et al. (2013).

Table 1. Continued

Group:	Pre-SVC1	Pre-SVC1	Pre-SVC1	Pre-SVC1	Pre-SVC1	Pre-SVC1
Sample:	SL8325[a]	SL8330[a]	SL8332[a]	SL8340[a]	SL8341[d]	SL8342[d]
SiO_2	55.76	55.88	57.31	53.46	61.38	50.90
TiO_2	1.52	1.15	0.64	0.77	0.53	0.76
Al_2O_3	15.12	15.38	18.99	19.19	16.62	22.11
FeO tot	10.73	11.04	8.04	8.93	7.66	7.75
MnO	0.20	0.22	0.25	0.20	0.22	0.20
MgO	3.51	3.68	2.20	3.71	2.10	2.72
CaO	7.41	7.48	7.70	9.24	6.09	11.68
Na_2O	3.36	3.22	3.45	2.96	3.71	2.51
K_2O	1.00	0.58	0.34	0.46	0.68	0.43
P_2O_5	0.21	0.14	0.18	0.08	0.15	0.08
LOI	3.49	2.22	2.47	0.76	1.99	1.43
Ti	13800	10280	5959	7212	4887	6973
V	348	296	51.9	198	52	207
Ga	17.2	16.4	17.2	16.9	15.4	16.7
Rb	15.9	11.1	5.71	12.9	20.9	10.0
Sr	190	173	238	205	228	221
Y	38.7	28.4	24.4	19.9	21.7	16.9
Zr	134	81.3	81.0	54.3	65.4	43.6
Nb	3.85	1.96	2.87	1.68	2.58	1.20
Ba	226	150	100	129	157	79.4
La	7.24	4.58	5.02	3.95	5.54	2.80
Ce	18.1	11.6	13.0	9.51	13.6	7.10
Pr	3.05	2.01	2.26	1.60	2.25	1.25
Nd	15.2	10.4	11.5	7.80	10.9	6.44
Sm	4.46	3.21	3.25	2.31	2.94	1.98
Eu	1.32	1.12	1.22	0.88	1.01	0.79
Gd	5.63	4.11	3.76	2.91	3.38	2.58
Tb	1.01	0.75	0.65	0.53	0.58	0.46
Dy	6.38	4.84	4.11	3.41	3.64	2.99
Ho	1.38	1.05	0.89	0.74	0.77	0.64
Er	3.87	2.93	2.51	2.05	2.17	1.79
Tm	0.65	0.49	0.43	0.34	0.38	0.30
Yb	4.02	2.99	2.80	2.17	2.40	1.81
Lu	0.64	0.49	0.47	0.35	0.40	0.29
Hf	3.65	2.28	2.16	1.59	1.85	1.30
Ta	0.29	0.16	0.20	0.13	0.19	0.11
Pb	5.05	6.19	3.54	2.62	3.50	1.67
Th	1.71	0.94	0.72	0.96	0.78	0.49
U	0.86	0.52	0.39	0.44	0.44	0.27
La/Sm	1.63	1.42	1.55	1.71	1.88	1.41
Th/Th*	0.58	0.51	0.55	0.61	0.45	0.52
$^{143}Nd/^{144}Nd$	0.512946	–	–	–	0.512958	0.512983
1 SE	0.000015	–	–	–	0.000003	0.000008
$^{87}Sr/^{86}Sr$	0.704394	–	–	–	0.704354	0.704174
1 SE	0.000006	–	–	–	0.000003	0.000003
$^{206}Pb/^{204}Pb$	19.291	–	–	–	–	–
1 SE	0.001	–	–	–	–	–
$^{207}Pb/^{204}Pb$	15.748	–	–	–	–	–
1 SE	0.001	–	–	–	–	–
$^{208}Pb/^{204}Pb$	38.930	–	–	–	–	–
1 SE	0.003	–	–	–	–	–
$^{176}Hf/^{177}Hf$	0.283027	–	–	–	0.283081	0.283032
1 SE	0.000002	–	–	–	0.000007	0.000009

Major element concentrations are from Davidson (1987) and Lindsay et al. (2013) and normalised to 100% volatile free. Sr, Nd and Pb isotope ratios are from Bezard et al. (2014). 1 SE = 1 standard error.

[a] Trace element concentrations and $^{176}Hf/^{177}Hf$ (if available) analysed at Durham University.

[b] Trace element concentrations analysed at Macquarie University and $^{176}Hf/^{177}Hf$ analysed at Durham University.

[c] Trace element concentrations and $^{176}Hf/^{177}Hf$ analysed at Macquarie University.

[d] Trace element concentrations analysed at Durham and $^{176}Hf/^{177}Hf$ analysed at Macquarie University.

*Also analysed by LA-ICPMS by Lindsay et al. (2013).

Table 1. Continued

Group:	Pre-SVC1	Pre-SVC1
Sample:	SL8344[a]	SL8345[d]
SiO_2	51.77	71.88
TiO_2	0.78	0.28
Al_2O_3	18.87	13.44
FeO tot	8.41	4.23
MnO	0.18	0.17
MgO	5.14	0.21
CaO	11.02	2.37
Na_2O	2.47	4.97
K_2O	0.34	1.92
P_2O_5	0.09	0.05
LOI	0.95	2.49
Ti	6974	2507
V	236	0.52
Ga	15.5	17.3
Rb	7.71	45.2
Sr	178	103
Y	17.6	57.6
Zr	49.4	209
Nb	1.11	4.71
Ba	79.6	324
La	3.34	12.3
Ce	8.08	29.4
Pr	1.36	4.93
Nd	6.75	23.6
Sm	2.03	6.62
Eu	0.74	1.39
Gd	2.57	7.89
Tb	0.46	1.44
Dy	2.98	9.34
Ho	0.65	2.01
Er	1.80	5.76
Tm	0.30	1.01
Yb	1.92	6.32
Lu	0.31	1.03
Hf	1.41	6.02
Ta	0.11	0.36
Pb	2.31	6.39
Th	0.70	3.30
U	0.28	2.01
La/Sm	1.65	1.86
Th/Th*	0.71	0.59
$^{143}Nd/^{144}Nd$	0.512957	0.512975
1 SE	0.000008	0.000002
$^{87}Sr/^{86}Sr$	0.704132	0.704109
1 SE	0.000002	0.000003
$^{206}Pb/^{204}Pb$	19.341	_
1 SE	0.001	_
$^{207}Pb/^{204}Pb$	15.747	_
1 SE	0.001	_
$^{208}Pb/^{204}Pb$	39.110	_
1 SE	0.003	_
$^{176}Hf/^{177}Hf$	0.283116	0.283156
1 SE	0.000006	0.000002

Major element concentrations are from Davidson (1987) and Lindsay et al. (2013) and normalised to 100% volatile free. Sr, Nd and Pb isotope ratios are from Bezard et al. (2014).

1 SE = 1 standard error.

[a] Trace element concentrations and $^{176}Hf/^{177}Hf$ (if available) analysed at Durham University.

[b] Trace element concentrations analysed at Macquarie University and $^{176}Hf/^{177}Hf$ analysed at Durham University.

[c] Trace element concentrations and $^{176}Hf/^{177}Hf$ analysed at Macquarie University.

[d] Trace element concentrations analysed at Durham and $^{176}Hf/^{177}Hf$ analysed at Macquarie University.

*Also analysed by LA-ICPMS by Lindsay et al. (2013).

Table 2. Least squares models to produce a residual melt with Pre-SVC1 andesite (SL-83-41; model #3), or SVC andesite (SL-83-17; models #1 and #2) compositions from differentiation of Pre-SVC1 basalt (SL-83-44) and the corresponding Rayleigh fractionation models.

#1	Init. mag. **SL-83-44**	Final mag. **SL-83-17**	Phase analyses (normalized to 100%) **Plag1**	**Opx1**	**Ilm1**	**Cpx1**
SiO_2	52.35	61.96	49.77	50.29	0.00	60.94
TiO_2	0.78	0.62	0.04	0.11	53.01	0.44
Al_2O_3	19.08	18.21	31.5	0.59	0.12	5.02
FeOt	8.51	5.36	0.79	27.71	45.51	4.51
MgO	5.20	2.62	0.10	20.45	1.27	0.12
CaO	11.14	6.78	13.32	0.84	0.02	28.76
Na_2O	2.50	2.73	3.98	0.01	0.00	0.21
K2O	0.34	1.58	0.14	0.00	0.01	0.00
P_2O_5	0.09	0.14	0.35	0.00	0.07	0.00
Total	100	100	100	100	100.01	100
∑(R^2)		**Res. Melt (%)**	**Phase (in % relative to initial magma)**			
0.03		14.27	50.13	23.02	1.10	11.48

#2	Init. mag. **SL-83-44**	Final mag. **SL-83-17**	Phase analyses (normalized to 100%) **Plag1**	**Opx1**	**Ilm1**	**Cpx1**	**Am1**
SiO_2	52.35	61.96	49.77	50.29	0	60.94	42.24
TiO_2	0.78	0.62	0.04	0.11	53.01	0.44	1.85
Al_2O_3	19.08	18.21	31.5	0.59	0.12	5.02	15.45
FeOt	8.51	5.36	0.79	27.71	45.51	4.51	8.63
MgO	5.2	2.62	0.1	20.45	1.27	0.12	16.53
CaO	11.14	6.78	13.32	0.84	0.02	28.76	12.77
Na_2O	2.5	2.73	3.98	0.01	0	0.21	2.08
K_2O	0.34	1.58	0.14	0	0.01	0	0.45
P_2O_5	0.09	0.14	0.35	0	0.07	0	0
	100	100	100	100	100	100	100
∑(R^2)		**Res. Melt (%)**	**Phase (in % relative to initial magma)**				
0.02		14.96	49.28	22.44	1.11	11.31	0.90

#3	Init. mag. **SL-83-44**	Final mag. **SL-83-41**	Phase analyses (normalized to 100%) **Plag2**	**Cpx2**	**Opx2**	**Ilm2**
SiO_2	52.35	62.04	49.88	51.2	50.77	0.27
TiO_2	0.78	0.54	0.04	0.37	0.41	16.14
Al_2O_3	19.08	16.8	30.86	3.25	1.36	2.15
FeOt	8.51	7.75	0.83	6.82	21.71	80.52
MgO	5.20	2.12	0.11	16.56	23.45	0.78
CaO	11.14	6.16	14.47	21.6	2.29	0.12
Na_2O	2.50	3.75	3.39	0.2	0.01	0.01
K_2O	0.34	0.69	0.10	0.00	0.00	0.01
P_2O_5	0.09	0.15	0.32	0.00	0.00	0.00
Total	100	100	100	100	100	100
∑(R^2)		**Res. Melt (%)**	**Phase (in % relative to initial magma)**			
0.05		31.27	42.65	12.85	9.94	3.29

Rayleigh fractionation model:

	La/Yb	La/Sm	Th/Th*
SL-83-44	1.74	1.65	0.71
SL-83-17	11.31	5.74	0.96
SL-83-41	2.31	1.88	0.45
#1 res. Melt	2.31	1.82	0.72
#2 res. Melt	2.29	2.02	0.72
#3 res. Melt	2.19	1.90	0.71

Table 3. Mineral-melt distribution coefficients used for Rayleigh fractionation and AFC models.

	Plag	Cpx	Opx	Ilm	Hbl
La	0.035	0.105	0.002	0.098	0.544
Nd	0.018	0.287	0.030	0.140	1.340
Sm	0.013	0.477	0.050	0.150	1.804
Yb	0.016	0.601	0.340	0.170	1.642
Hf	0.009	0.121	0.010	0.380	1.534
Sr	1.670	0.070	0.040	0.010	0.480
Pb	0.36	0.0102	0.0013	0.01	0.1
Ba	0.29	0.001	0.011	0.00034	0.16
U	0.25	0.01	0.0046	0.0082	0.004
Th	0.25	0.012	0.0012	0.00055	0.004

Distribution coefficients were compiled from Aignertorres et al. (2007), Arth (1976), Paster et al. (1974), Dostal (1983), Fujimaki et al. (1984), Green et al. (1989), McKenzie and O'Nions (1991), Salters and Longhi (1991) and Zack and Brumm (1998) and set to 0.01 where not available and known to be insignificant. Plag = Plagioclase, Cpx = clinopyroxene, Opx = orthopyroxene, Ilm = ilmenite; Hbl = hornblende.